Mid-Cretaceous orogenic gold and molybdenite mineralization in the Independence Creek area, Dawson Range, parts of NTS 115J/13 and 14

Greg G. McKenzie, Murray M. Allan[1], James K. Mortensen, Craig J.R. Hart, Matías Sánchez
Mineral Deposit Research Unit, University of British Columbia, Vancouver, BC

Robert A. Creaser[2]
Department of Earth & Atmospheric Sciences, University of Alberta, Edmonton, AB

McKenzie, G.G., Allan, M.M., Mortensen, J.K., Hart, C.J.R., Sánchez, M., and Creaser, R.A., 2013. Mid-Cretaceous orogenic gold and molybdenite mineralization in the Independence Creek area, Dawson Range, parts of NTS 115J/13 and 14. *In:* Yukon Exploration and Geology 2012, K.E. MacFarlane, M.G. Nordling, and P.J. Sack (eds.), Yukon Geological Survey, p. 73-97.

ABSTRACT

The Boulevard gold prospect, located in the Independence Creek area of the Dawson Range, comprises sheeted, auriferous quartz-sulphide-carbonate veins and fault breccia, hosted mainly by mafic schist. The nearby Toni Tiger molybdenum showing is characterized by quartz-molybdenite veins cutting Late Permian meta-aplite and garnet-pyroxene skarn of uncertain age. We present geochronological evidence that gold and molybdenum were deposited at 96-95 Ma, approximately 3 m.y. after intrusion of the Dawson Range batholith and Coffee Creek granite. Fluid inclusions from mineralized quartz veins suggests that gold at Boulevard and molybdenite at Toni Tiger were formed from similar H_2O-CO_2-NaCl type fluids between 279 and 310°C and >1 kbar. We conclude that both are part of the same mineralizing system, and that structurally-hosted gold at the nearby Coffee deposit and in the Moosehorn Range of western Yukon may be broadly related, post-arc orogenic systems developed during exhumation of the Dawson Range in mid-Cretaceous time.

[1] *mallan@eos.ubc.ca*

INTRODUCTION

The Independence Creek area is a broad upland plateau within the Dawson Range of west-central Yukon, and is incised by stream systems draining north into the Yukon River. The area is located approximately 140 km south of Dawson, 40 km south of the Golden Saddle gold deposit (Kinross Gold Corp.), which contains 1.4 Moz of gold (Underworld Resources Inc., January 19, 2010 press release), and approximately 10 km southwest of the Coffee gold deposit, which contains 3.2 Moz of gold (Kaminak Gold Corp., December 13, 2012 press release) (Fig. 1).

Gold mineralization of the Boulevard zone was first identified by Rimfire Minerals Corp. in 2007 in the headwaters of the Independence Creek drainage. It is a northwest-trending, 450 m by 1.2 km, gold-arsenic-antimony soil geochemical anomaly with sporadic tellurium and bismuth. Exploration at Boulevard was pursued further by Rimfire in 2008, Silver Quest Resources Ltd. from 2009 to 2011, and Independence Gold Corp. in 2012. Exploration methods at Boulevard have included stream sediment geochemistry, soil geochemistry, trenching, mapping, prospecting, induced polarization and magnetometry surveys, airborne aeromagnetic and radiometric surveys, and diamond drilling.

The Toni Tiger molybdenum showing (Yukon MINFILE 115J 052) is located approximately 2 km east of the Boulevard trend (Fig. 2). Mineralization was discovered by regional silt survey in 1969 by Archer, Cathro and Associates, and the anomaly was attributed to disseminated molybdenite in skarn with associated

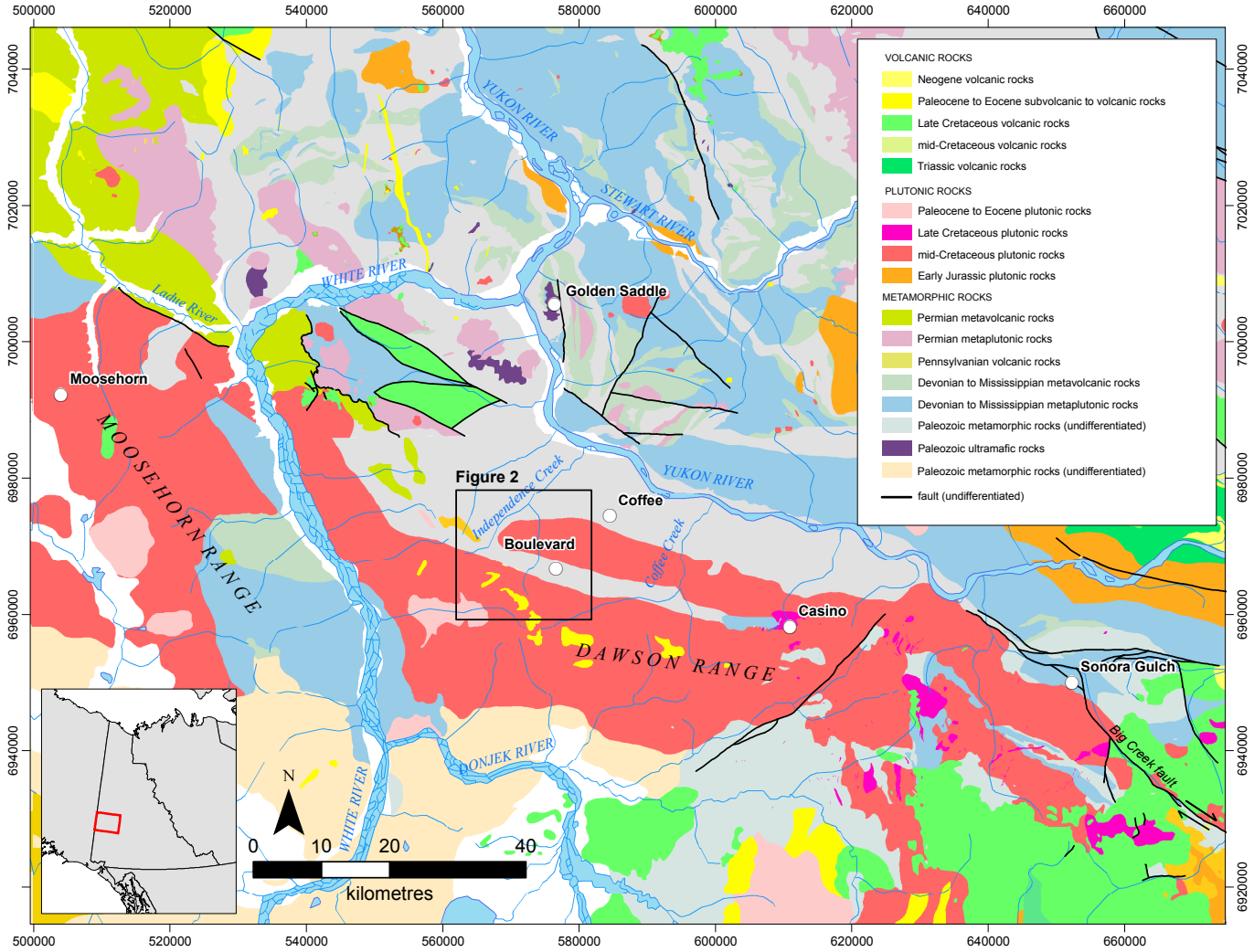

Figure 1. *Geological map of the Dawson Range (in greater Yukon Plateau), showing significant mineral deposits and prospects (geology modified from Gordey and Ryan (2005) and Gordey and Makepeace (2003)). The Independence Creek study area is indicated by the black box. Datum: NAD83; Projection: UTM zone 7N.*

chalcopyrite, arsenopyrite, scheelite, and pyrite (Craig, 1970). Trenching at the prospect exposed quartz-molybdenite veins, and Craig (1970) inferred that molybdenite was associated with, and restricted to, the skarn alteration.

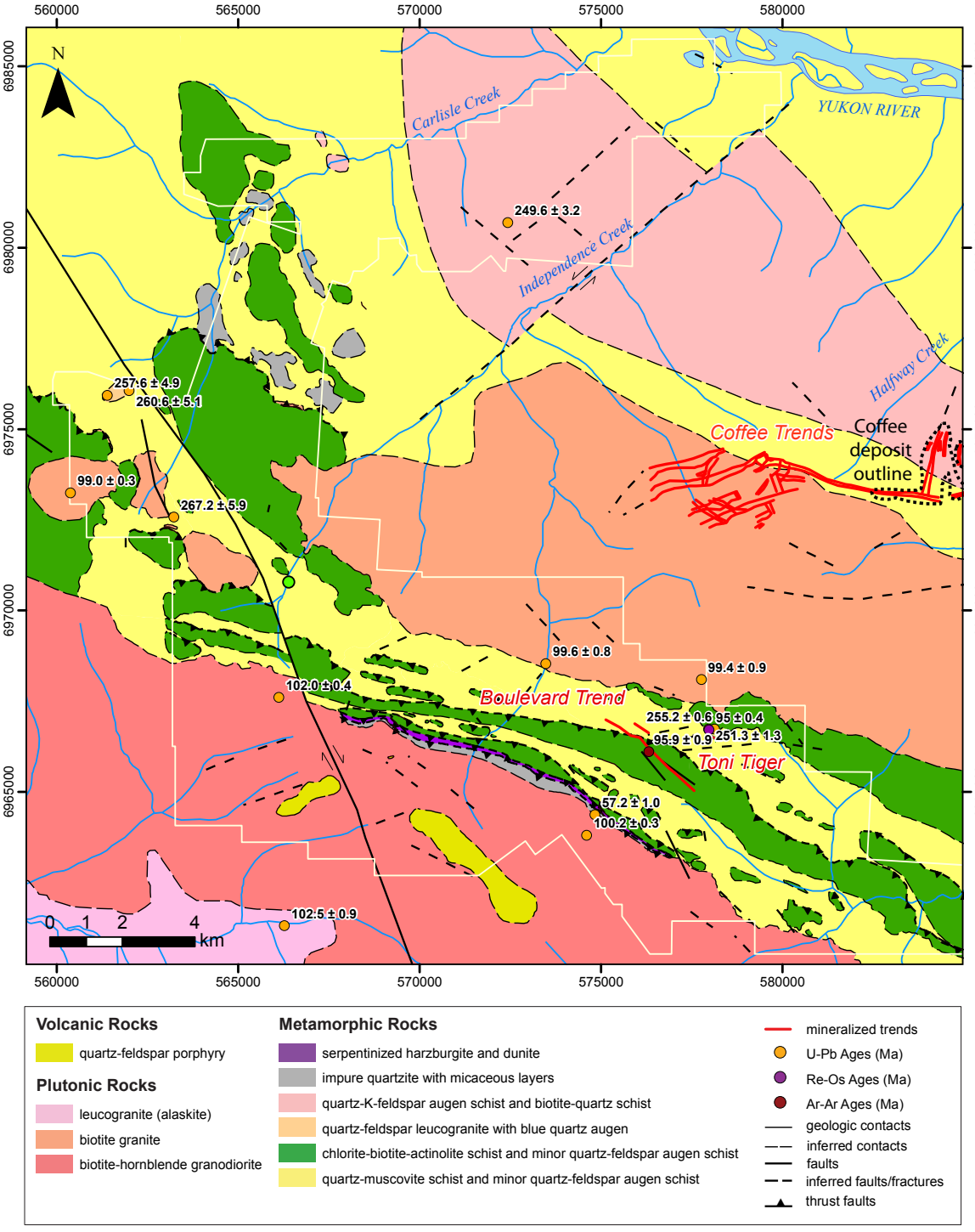

Figure 2. *Geologic map of the Independence Creek area, showing geochronological data and mineralized trends in the Boulevard and Coffee prospects (Datum: NAD83; Projection: zone 7N). Additional sources of information include: Tempelman-Kluit, 1974; Jilson, 2000; Gordey and Ryan, 2005; Chartier et al., 2013; J. Ryan, pers. comm., 2012. The white line defines Silver Quest property limits as of June 2011.*

The Boulevard and Toni Tiger prospects present an opportunity to investigate the age and geological characteristics of two proximal mineralized systems that have contrasting metal associations (Au-As-Sb and Mo-Cu-W, respectively) and uncertain metallogenesis. The geologic relationships presented below are based on mapping, interpretations of airborne magnetic and radiometric data, and detailed observations of diamond drill core. We present U-Pb zircon ages both for metamorphic rocks (including those hosting molybdenite mineralization), and for samples of the Dawson Range batholith, Coffee Creek plutonic suite, and local subvolcanic units. Petrographic observations and reconnaissance-level fluid inclusion data from mineralized veins are also included. Finally, we present $^{40}Ar/^{39}Ar$ muscovite ages for gold-bearing veins at Boulevard and Re-Os molybdenite ages for Toni Tiger, both of which are interpreted to date mineralization directly.

FIELD RELATIONSHIPS

GEOLOGY

The Independence Creek area is underlain by a 3 km-wide, west-northwest-trending belt of predominantly schistose and gneissic rocks (Figs. 1, 2 and 3). This rock package includes the following map units (Fig. 2): (a) serpentinized harzburgite and dunite; (b) variably pyritic chlorite-biotite-actinolite schist, containing minor quartz-feldspar augen schist; (c) quartz-muscovite schist, containing minor calcareous schist; (d) impure quartzite with micaceous layers; (e) foliated quartz-feldspar-muscovite leucogranite and quartz-feldspar augen schist with distinctive blue quartz augen; and (f) quartz-K-feldspar augen schist and minor biotite-quartz schist. Peak metamorphic grade is inferred to be middle greenschist facies on the basis of biotite-chlorite-actinolite assemblages in mafic schists. Lithological heterogeneities are common on the scale of metres to hundreds of metres, due to a combination of original stratigraphic and intrusive contact relationships, and repetition by tight to isoclinal folding and faulting. Ultramafic rocks are exposed as small lenticular bodies near the south margin of the metamorphic package (Figs. 2 and 3f), and are inferred to delineate a major crustal-scale fault (Templeman-Kluit, 1974; Gordey and Makepeace, 2003; Zagorevski *et al.*, 2012).

The metamorphic package is intruded to the south by medium to coarse-grained biotite-hornblende granodiorite of the Dawson Range batholith, a phase of the mid-Cretaceous Whitehorse plutonic suite (Figs. 1, 2, and 3a). The rock is massive to lineated with locally aligned hornblende and stretched quartz. To the north, metamorphic rocks are intruded by the Coffee Creek phase of the Whitehorse plutonic suite (Templeman-Kluit, 1974), which is composed of medium to coarse-grained biotite granite with volumetrically minor aplitic and pegmatitic phases (Figs. 1, 2, and 3b). A garnet-bearing, quartz-phyric porphyry phase is recognized at the western tip of the Coffee Creek granite. No crosscutting relationships are observed between plutonic rocks and gold mineralization at Boulevard or molybdenite-bearing veins at Toni Tiger.

Locally, subcrop of porphyritic rhyodacite and basalt are observed near the northern margin of the Dawson Range batholith (unit too small to represent on Fig. 2). This unit has been mapped and interpreted as a hypabyssal intrusion (J. Ryan, pers. comm., 2012).

STRUCTURES

The principal fabric within metamorphic rock units in the study area strikes 280-290°N and is steeply dipping between ~70 and 90°. West of the Coffee Creek granite, the strike of the regional metamorphic fabric rotates to 315°N (Fig. 2). This structural pattern in the metamorphic rocks mirrors a major change in the regional strike of the Dawson Range batholith approximately 20 km west of the study area (Fig. 1).

The main metamorphic fabric has strongly transposed any original depositional features within the metamorphic rock units. The development of this fabric is likely due to D_1 and D_2 collisional deformation accompanying peak metamorphism of Yukon-Tanana terrane rocks in Late Permian time (Berman *et al.*, 2007; MacKenzie *et al.*, 2008a; Beranek and Mortensen, 2011). Isoclinal, rootless fold hinges and boudinaged quartz veins are interpreted to represent D_2 phase folds that overprint the earlier S_1 fabric.

A third deformation event (D_3) can be recognized as locally developed crenulations (S_3) and tight disharmonic folding of the pre-existing metamorphic fabric, and is best developed within micaceous lithologies. These folds have axial traces that are subparallel to the regional west-northwest map trend of the metamorphic rock package and axial planes that are subvertical. Ultramafic bodies along the northern margin of the Dawson Range define a lineament that extends eastward toward the Casino Cu-Mo-Au porphyry deposit and the Sonora Gulch porphyry prospect (Fig. 1), and are interpreted to define a crustal-

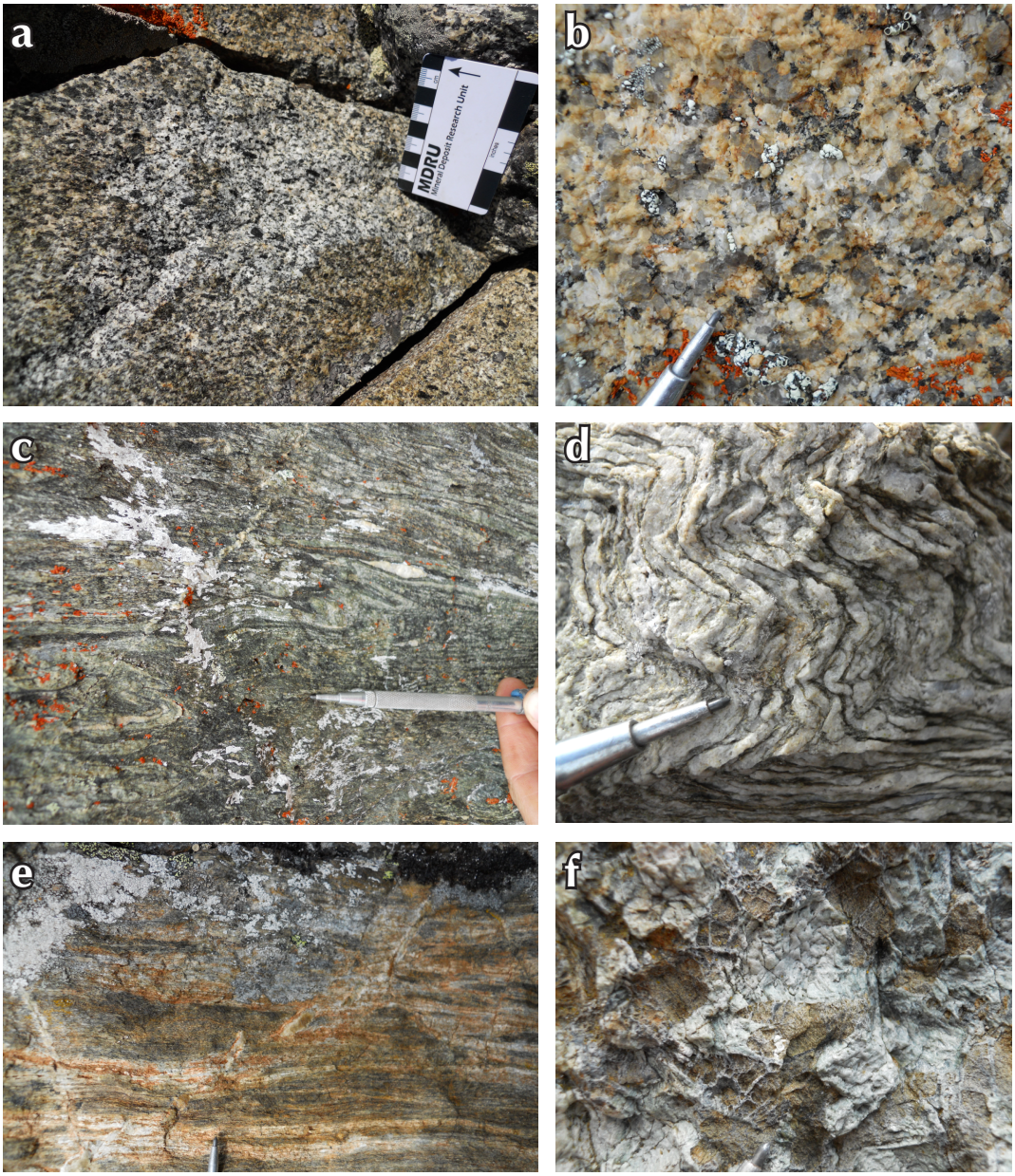

Figure 3. *Typical rock types in the Independence Creek area: (a) biotite hornblende granodiorite of the Dawson Range batholith; (b) biotite granite of the Coffee Creek granite; (c) strongly deformed chloritic schist (typical host rock to gold mineralization); (d) folded metagranite; (e) banded diopside-garnet skarn and biotite schist (typical host rock at the Toni Tiger molybdenum showing); and (f) serpentinitzed harzburgite.*

scale fault that was partially intruded by the Dawson Range batholith (Zagorevski *et al.*, 2012). The origin of this structure is uncertain, but it was likely active in the Early Jurassic, when regional scale thrust faulting imbricated slivers of Slide Mountain oceanic crust within the Yukon-Tanana terrane (MacKenzie *et al.*, 2008a,b; MacKenzie and Craw, 2012).

Locally-developed stretching lineations within the Dawson Range batholith are subhorizontal and parallel to the regional west-northwest strike of metamorphic rocks to the north. The Coffee Creek granite is almost entirely massive, suggesting that either fabrics in the Dawson Range batholith were formed prior to emplacement of the Coffee Creek granite, or that syn to post-magmatic deformation was partitioned more strongly in the Dawson Range batholith.

A fault trending 330°N is obvious in aeromagnetic data, and cuts the metamorphic package and the Dawson Range batholith with 1 km of dextral offset (southwest quadrant of Fig. 2). This fault is the most prominent in a series of northwest to north-northwest-trending structures that truncate the west-northwest-trending magnetic grain of the metamorphic package (Fig. 2). A similar northwest to north-northwest orientation is observed for gold-bearing structures at the Boulevard prospect. The offset of the northern intrusive contact of the Dawson Range batholith by this fault generation indicates that this fault set occurred after emplacement of the Dawson Range batholith in mid-Cretaceous time.

VEINS, ALTERATION, AND MINERALIZATION

Observations on veining, alteration, and mineralization are presented for the Boulevard and Toni Tiger prospects separately, since field relationships do not provide sufficient information about the relative timing of these adjacent systems.

BOULEVARD

Detailed observations of diamond drill core reveal five separate vein generations (Fig. 4), all of which are hosted primarily in biotite-chlorite ± actinolite schist. A paragenetic scheme is presented in Figure 5 and petrographic observations are shown in Figure 6.

V_1: The first vein generation (V_1) comprises sugary quartz ± pyrite veins, and is found in all metamorphic rock types in the study area (Fig. 4a). V_1 veins are typically ~1 cm wide and contain less than 1% pyrite and trace chalcopyrite as inclusions in pyrite. V_1 veins are conformable with the metamorphic fabric, and commonly occur as boudins and rootless hinges in mesoscopic folds. V_1 veins are early and are interpreted to be metamorphic segregations formed during Late Permian tectonism.

V_2: V_2 veins are composed of quartz, pyrrhotite ± chalcopyrite, are 5 to 30 mm wide, have irregular margins, and no alteration envelopes (Fig. 4b). V_2 veins are generally discordant to the S_1/S_2 fabric, suggesting they post-date peak deformation.

V_3: V_3 veins are composed mainly of quartz and ferroan carbonate with muscovite/illite-pyrite-arsenopyrite

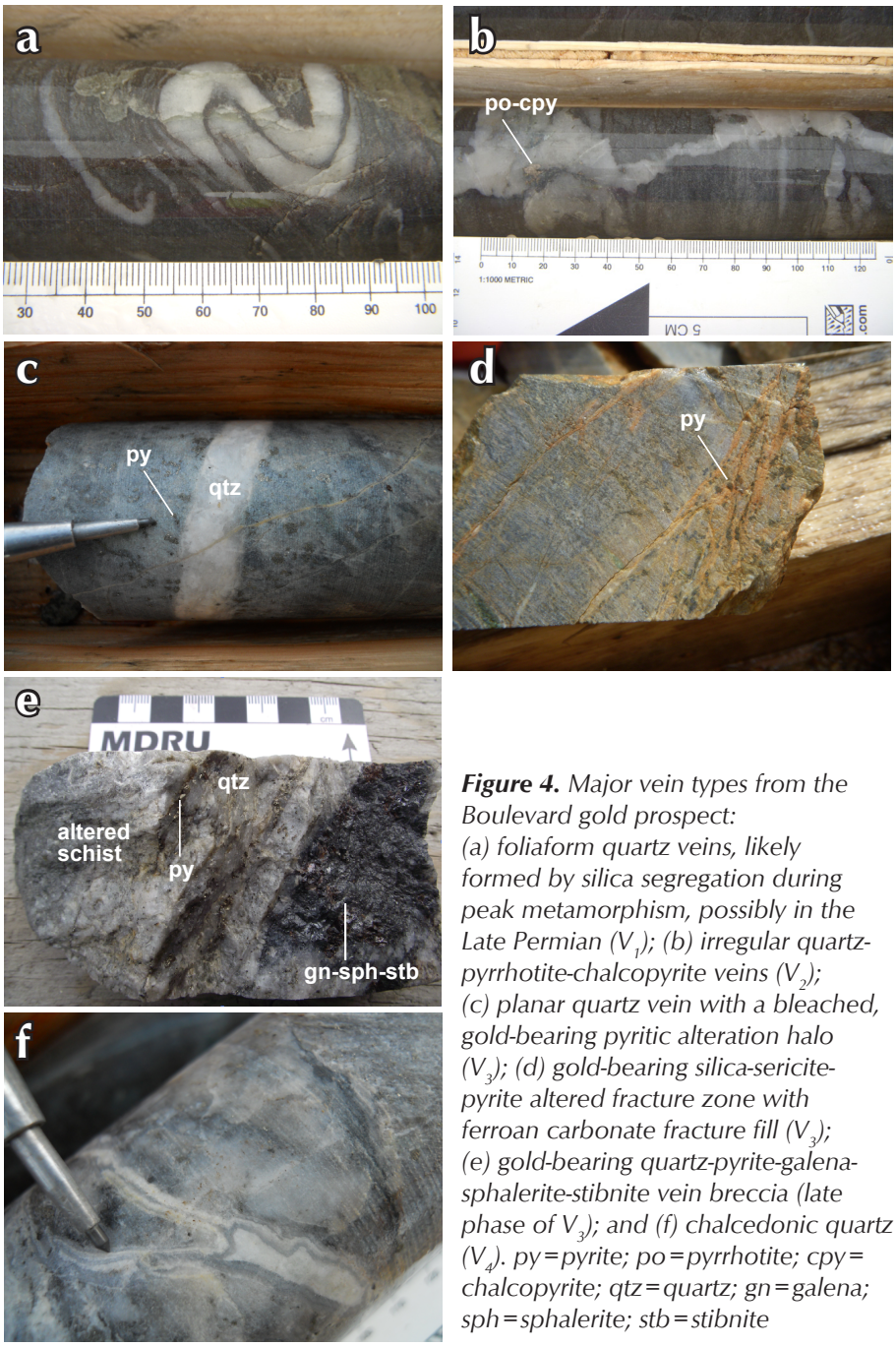

Figure 4. *Major vein types from the Boulevard gold prospect: (a) foliaform quartz veins, likely formed by silica segregation during peak metamorphism, possibly in the Late Permian (V_1); (b) irregular quartz-pyrrhotite-chalcopyrite veins (V_2); (c) planar quartz vein with a bleached, gold-bearing pyritic alteration halo (V_3); (d) gold-bearing silica-sericite-pyrite altered fracture zone with ferroan carbonate fracture fill (V_3); (e) gold-bearing quartz-pyrite-galena-sphalerite-stibnite vein breccia (late phase of V_3); and (f) chalcedonic quartz (V_4). py = pyrite; po = pyrrhotite; cpy = chalcopyrite; qtz = quartz; gn = galena; sph = sphalerite; stb = stibnite*

	V_1	V_2	V_3	V_4	V_5
quartz	———	———	———	———	
ferroan carbonate			———	———	———
pyrite	——	———	——— ——	———	
arsenopyrite			——		
gold			—— —		
pyrrhotite		———			
chalcopyrite	——	———			
sphalerite			—		
galena			—		
stibnite			—		
tetrahedrite			—		

Figure 5. *Mineral paragenesis for veins present in the Boulevard gold prospect.*

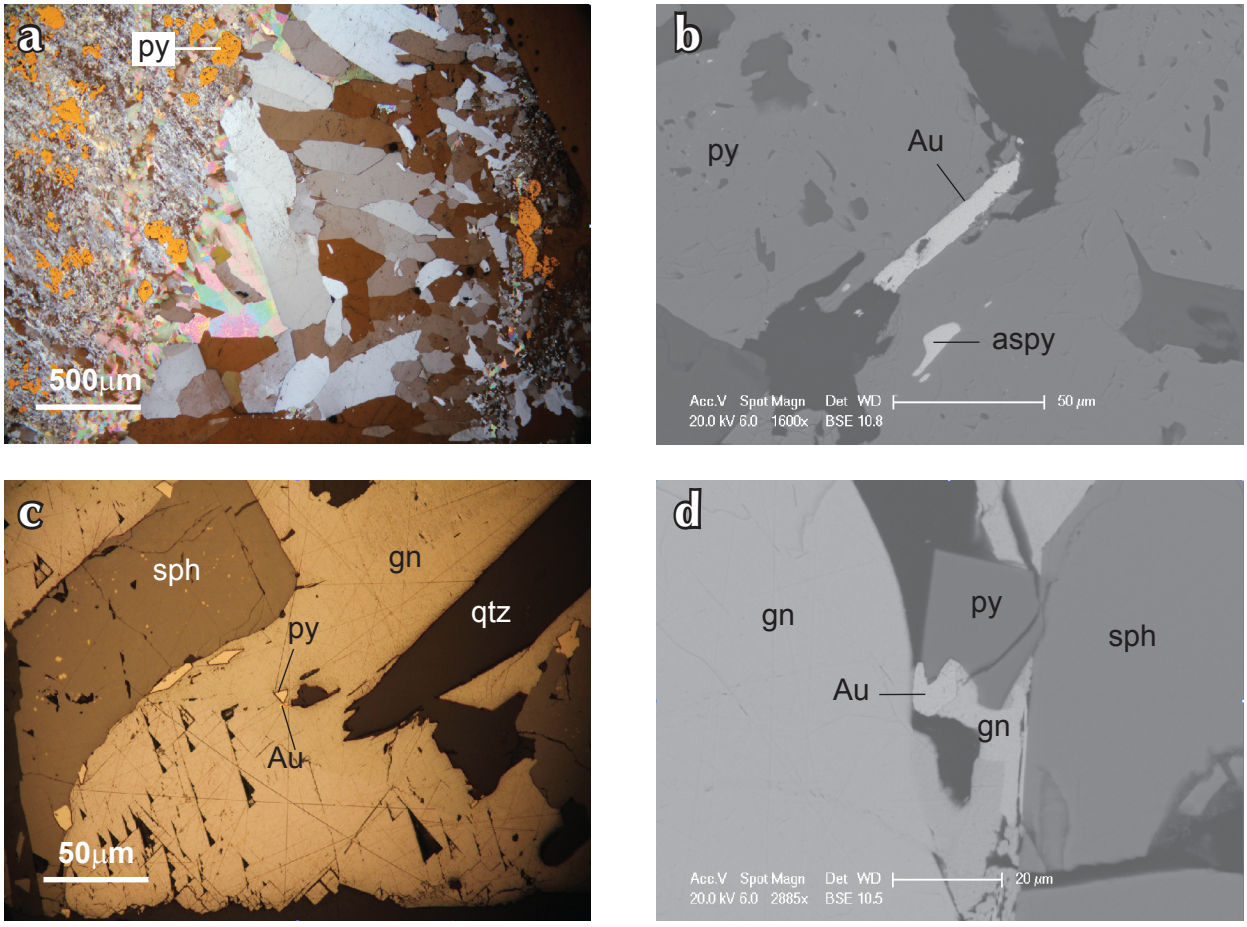

Figure 6. *Examples of gold mineralization from the Boulevard area: (a) typical V_3-generation quartz-carbonate vein with a gold-bearing pyrite halo (combined cross-polarized transmitted light and reflected light); (b) backscattered electron microscope image of gold associated with pyrite and arsenopyrite; (c) reflected light photomicrograph of a <5 µm gold grain as an inclusion in galena; (d) backscattered electron microscope image of a 10 µm gold grain associated with galena, sphalerite and pyrite. aspy = arsenopyrite (other mineral abbreviations as in Figure 4).*

alteration envelopes (Figs. 4c,d, 6a, and 8a). A paragenetically late phase of sphalerite-galena-pyrite-tetrahedrite ± stibnite is observed in some veins, especially where brecciation has also taken place (Fig. 4e). Veins are typically 2 to 20 mm wide, planar, and occur in sheeted sets that cut the S_1/S_2 fabric at a high angle. Approximations of vein orientations (using the local metamorphic fabric as a reference plane in unoriented drill core) yield a predominantly northwest strike and a dip of approximately 30° to the southwest. V_3 vein swarms are spatially related and subparallel to mineralized fault gouge. The faulting is interpreted to post-date V_3 veining since vein fragments have been noted in the fault gouge. Gold has two petrographic associations: (1) inclusions and fracture fillings in pyrite or arsenopyrite in alteration haloes (Fig. 6b); and (2) inclusions in sphalerite-galena-pyrite-tetrahedrite ± stibnite (Fig. 6c,d). Gold grains are typically less than 10 μm.

V_4: A fourth vein generation (V_4) is characterized by thin, colloform banded chalcedonic quartz-carbonate ± pyrite ± chalcopyrite veins (Fig. 4f). They vary in width from 5 to 60 mm. Carbonate is typically pink and manganiferous. V_4 veins crosscut both the metamorphic fabric and V_3 stage veins.

V_5: Thin (1-5 mm) ferroan carbonate veinlets (V_5) cut the metamorphic foliation and all pre-existing vein types. This vein generation has no known association with sulphides or gold.

TONI TIGER

The local host rocks include meta-aplite (Fig. 7a,b), biotite-quartz-feldspar schist (Fig. 7c-e), biotite hornfels, and garnet-diopside skarn (Fig. 7f). All rock types are cut by 1 cm to 1 m-wide, milky white quartz ± molybdenite veins (Figs. 7c-e and 8c) that occupy subvertical, conjugate fracture sets trending north and northeast. Molybdenite is also observed as wall rock disseminations in vein halos in biotite-quartz-feldspar schist and skarn. Veins have biotite-destructive chlorite-muscovite envelopes where they cut biotite-bearing host rocks (Fig. 7c,f). Idiomorphic garnet of hydrothermal origin is common along the margins of quartz ± molybdenite veins cutting the skarn unit.

FLUID INCLUSION PROPERTIES

BOULEVARD

Petrographic observations and a small number of microthermometric analyses were carried out on samples of quartz-hosted fluid inclusions from gold-stage V_3 veins at Boulevard. A homogenous population of aqueous-carbonic fluid was observed, which, based on clathrate melting and CO_2 homogenization temperatures, contains 15 to 24 mol % CO_2, ~2 to 3 wt % NaCl, and a bulk density of 0.8 to 0.85 g/cm³ (Fig. 8a,b). Homogenization temperatures and equation-of-state modeling, using the approach of Allan *et al.* (2011), suggest that fluids were trapped between 280 and 310°C or greater, at a pressure of 1100 bar or more. This pressure corresponds to a minimum depth of approximately 4.0 km at lithostatic pressures (assuming a rock density of 2800 kg/m³).

TONI TIGER

A homogenous population of aqueous-carbonic fluid inclusions was observed in vein quartz from Toni Tiger (Fig. 8c). Microthermometric measures of clathrate melting and CO_2 homogenization demonstrate that this fluid contains ~16 mol % CO_2 and ~3 wt % NaCl, with a bulk density of ~0.88 g/cm³ (Fig. 8d). Fluids were trapped at 280°C or more, at a minimum pressure of 1050 bar (>3.8 km at lithostatic pressure, assuming a rock density of 2800 kg/m³). The composition and trapping conditions of fluid inclusions from Toni Tiger veins are therefore indistinguishable from those in V_3 veins at Boulevard.

U-Pb GEOCHRONOLOGY

SAMPLES AND METHODOLOGY

U-Pb dating of zircon was used to determine the crystallization age of various units in the Independence Creek area, including the metamorphic rock package, Dawson Range batholith, Coffee Creek granite, and subvolcanic rocks. The sample suite includes six samples of metaplutonic rocks, including meta-aplite cut by quartz-molybdenite veins at Toni Tiger (I034207); orthogneiss containing minor disseminated molybdenite (I034224); and quartz-feldspar-biotite schist (GM11-9b, MA11-004BV, MA11-005BV, MA11-006BV). The suite also includes three samples of the Dawson Range batholith (I034239, YGR-BV-004, 99M-106-b); three samples of the Coffee Creek phase (YGR-BV-002, 99M-105, 99M-107); and a single sample of quartz-feldspar rhyodacite porphyry (MA11-001BV).

Zircon grains recovered from plutonic and metaplutonic rocks are all relatively coarse grained (up to 200 μm long) and show a similar range of external morphology and internal structure. Zircons are typically clear, euhedral,

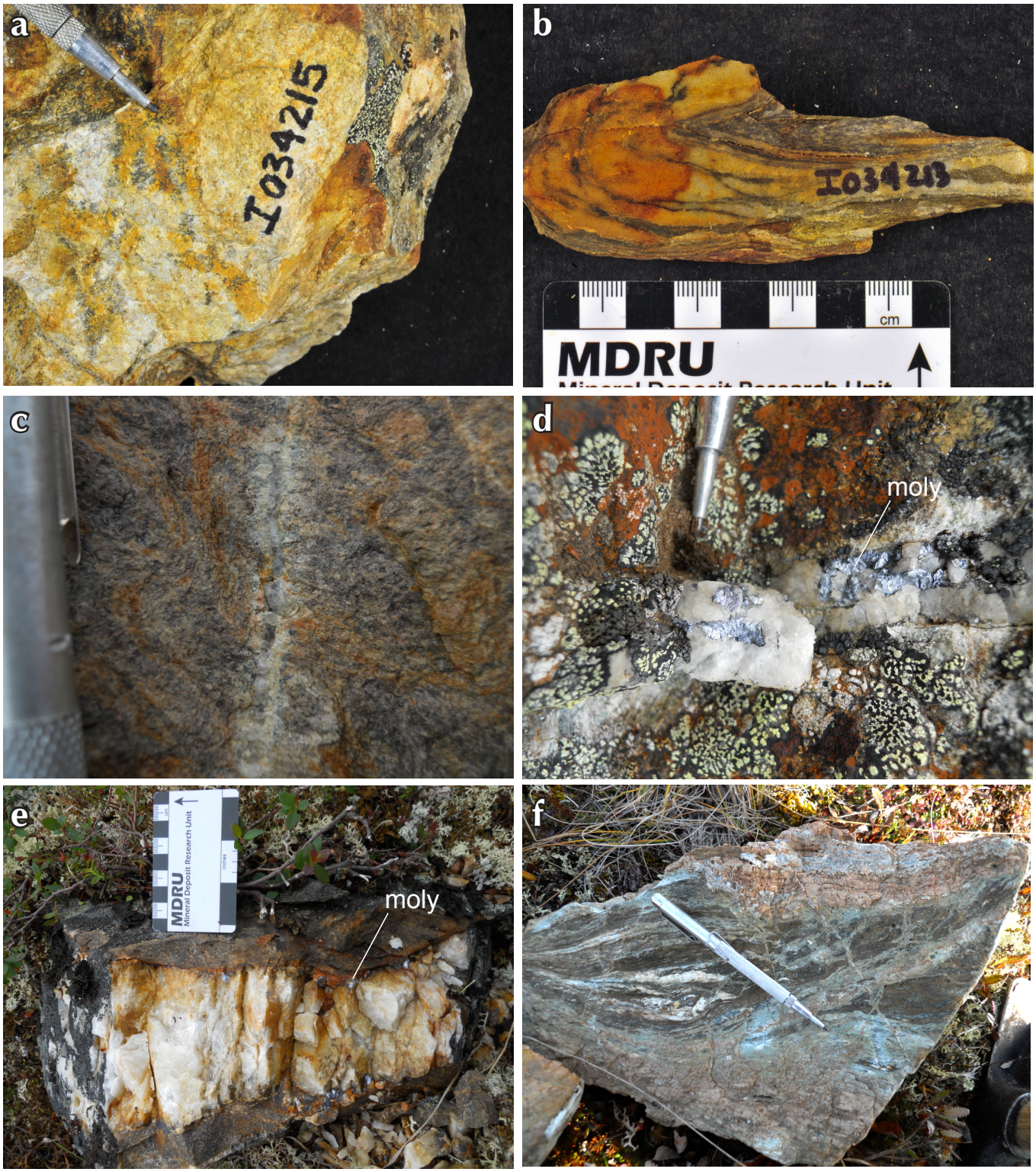

Figure 7. *Rock types and vein features of the Toni Tiger molybdenum occurrence: (a) weakly foliated meta-aplite from the Toni Tiger occurrence; (b) same meta-aplite as in (a), but interfoliated with biotite schist and affected by a later phase of folding; (c) biotite metagranitoid cut by a quartz-molybdenite vein with a chloritic alteration halo; (d) typical milky quartz vein with molybdenite from the Toni Tiger occurrence; (e) milky quartz vein with molybdenite along its margins (and as wall rock disseminations); and (f) pyroxene-garnet skarn with domains of biotite hornfels. moly=molybdenite.*

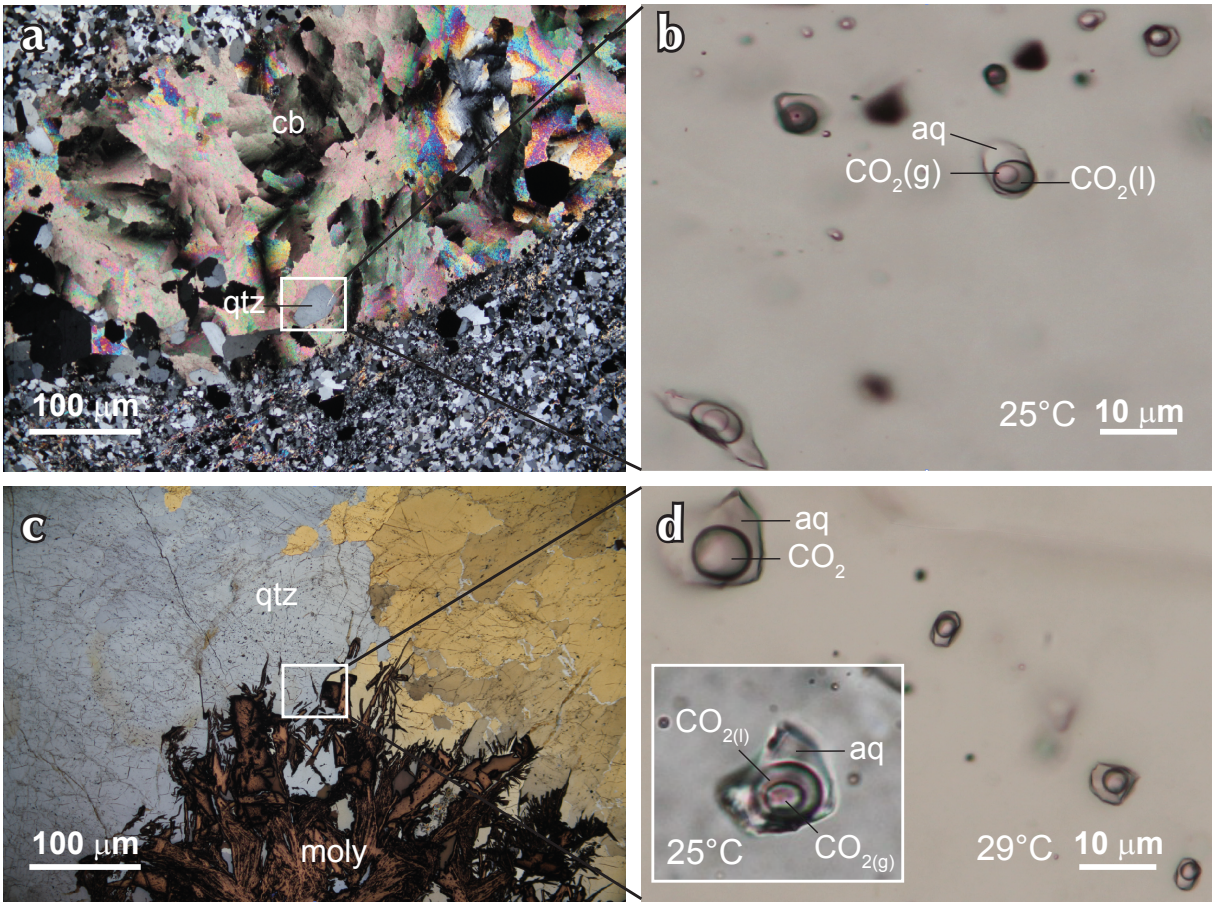

Figure 8. *(a) photomicrograph of a V_3-generation quartz-carbonate vein (cross-polarized light) from the Boulevard gold prospect; (b) quartz-hosted fluid inclusions from the vein in (a), containing aqueous liquid (aq), CO_2 liquid, and CO_2 vapour (photograph taken at 25°C); (c) photomicrograph of molybdenite in quartz from the Toni Tiger occurrence (combined cross-polarized transmitted light and reflected light); (d) photomicrograph of fluid inclusions in quartz associated with molybdenite mineralization in (c). Fluid inclusions contain aqueous liquid and a supercritical CO_2 phase (photograph taken just above the homogenization temperature of the carbonic liquid and vapour phase at 29°C). The inset shows both CO_2 phases below the homogenization temperature (~25°C), for the same large fluid inclusion in (d). cb=carbonate; g=gas phase; l=liquid phase; aq=aqueous phase (other abbreviations as in Figures 4 and 7).*

and colourless to pale yellow-brown. No obvious internal zoning was observed and morphologies range from stubby octahedral prisms to multi-faceted terminations.

The methodology for laser ablation ICP-MS analysis at the Pacific Centre for Isotopic and Geochemical Research (PCIGR), University of British Columbia, follows that described in Tafti *et al.* (2009) and Beranek and Mortensen (2011). The $^{206}Pb/^{238}U$ age is the most precisely determined age for the Phanerozoic zircons in question and is interpreted as the best estimate for the crystallization age of the samples. Assigned ages are based on a weighted average of overlapping, concordant $^{206}Pb/^{238}U$ ages of individual analyses for each sample. Errors are quoted at the 2σ level.

RESULTS

Results are presented in conventional U-Pb concordia plots and weighted average $^{206}Pb/^{238}U$ age summary plots in Figures 9-12 and are shown with sample locations in Table 1. Full analytical data are presented in Appendix 1.

All meta-igneous samples yielded Late Permian crystallization ages in the range of 250 to 267 Ma (Figs. 9 and 10). The molybdenite-bearing, weakly foliated meta-aplite sample (I034207) from Toni Tiger yields a well-constrained age of 251.3 ± 1.3 Ma (Fig. 9b), which suggests that this unit may be part of a post-D_2 intrusive suite of crustally derived intrusions that includes the Jim Creek pluton of the southern Klondike District (Beranek and

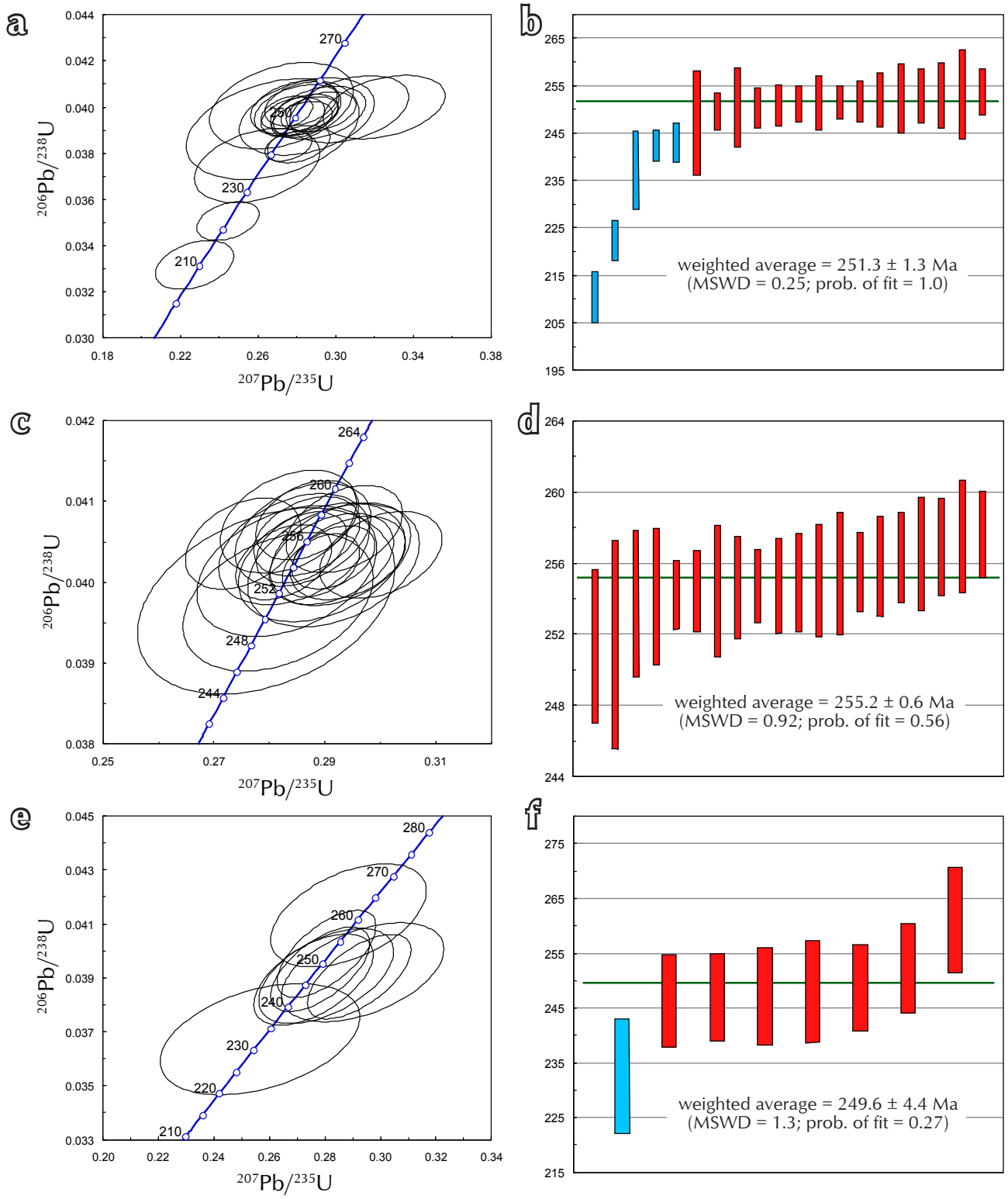

Figure 9. *Conventional concordia diagrams and plots of weighted average $^{206}Pb/^{238}U$ ages for meta-igneous samples from the study area: (a) and (b) sample I034207 – molybdenite-bearing meta-aplite from Toni Tiger; (c) and (d) sample I034224 - orthogneiss with disseminated molybdenite; (e) and (f) sample GM11-9b – quartz-feldspar-biotite schist. Error ellipses on concordia diagrams and error bars on weighted average age plots are shown at 2s level. Red bars on weighted average age plots were used in the age calculation; blue bars were rejected.*

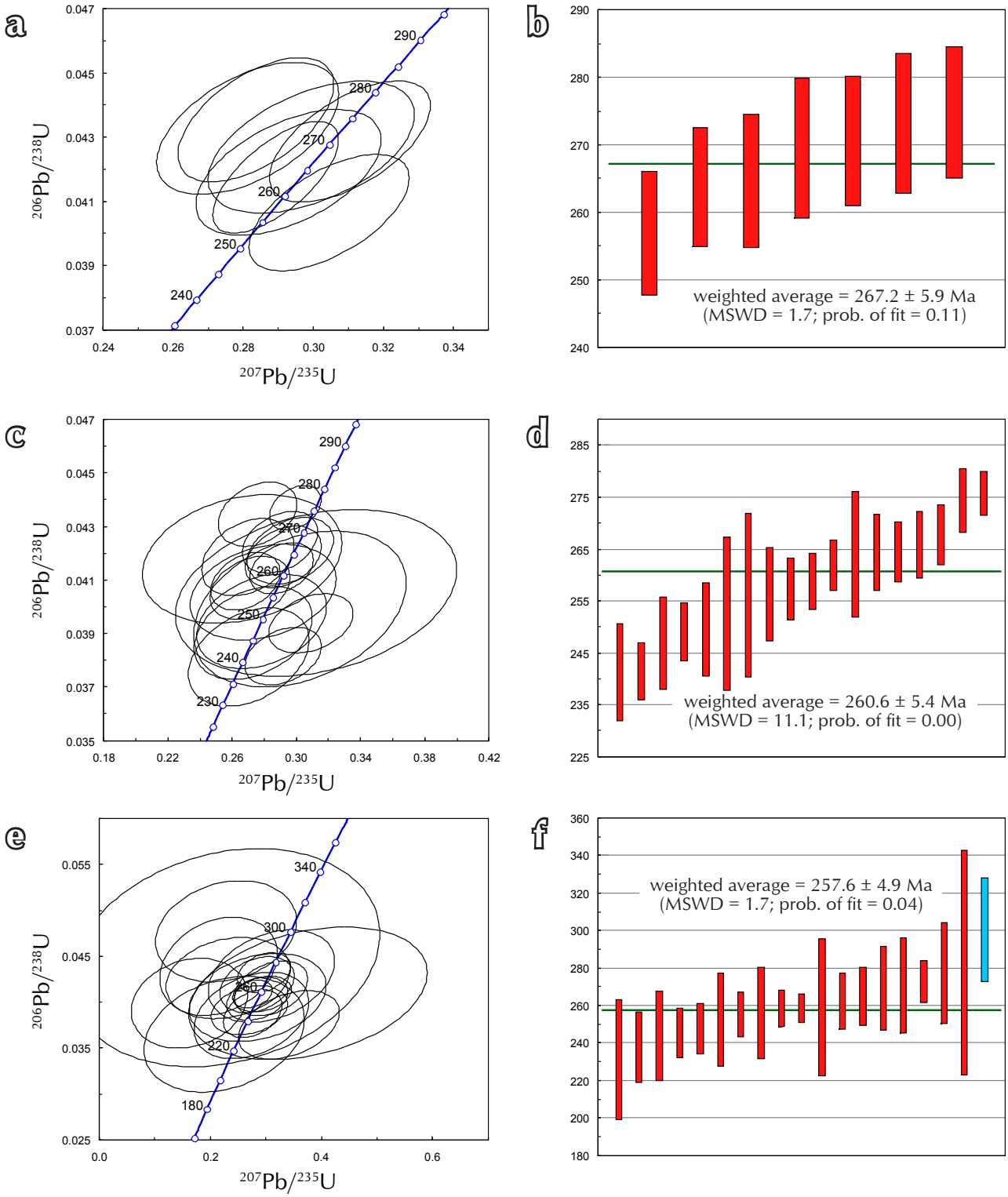

Figure 10. *Conventional concordia diagrams and plots of weighted average $^{206}Pb/^{238}U$ ages for meta-igneous samples from the study area: (a) and (b) sample MA11-004BV - quartz-feldspar-biotite schist; (c) and (d) sample MA11-00BV – quartz-feldspar-biotite schist; (e) and (f) sample MA11-006BV - quartz-feldspar-biotite schist. Symbols as in Figure 9.*

Mortensen, 2011) and the Teacher intrusion in the White Gold area (Mortensen, unpublished data). A sample of quartz-feldspar-biotite schist (GM11-9b) yields a similar age of 249.6±4.4 Ma (Fig. 9f); however, only a small amount of zircon was recovered from this sample and the age is therefore relatively imprecise (based on only seven analyses). All of the other well-foliated meta-igneous rock units yield Late Permian ages ranging from 255 to 267 Ma, which are consistent with ages reported elsewhere for metavolcanic and metaplutonic phases of the Klondike arc assemblage (Mortensen, 1990; Ruks *et al.*, 2006; Beranek and Mortensen, 2011).

Two samples of granodiorite from the Dawson Range batholith give ages of 102.0±0.4 Ma and 100.2±0.3 Ma (Fig. 11b,d). An aplite dyke that cuts Dawson Range granodiorite gives an age of 102.5±0.9 Ma (Fig. 11f). Three biotite granite samples of the Coffee Creek granite give ages ranging from 99 to 100 Ma (Fig. 12b,d,f). The ages are therefore consistent with the Coffee Creek granite being a slightly younger magmatic phase of the Whitehorse plutonic suite than the Dawson Range batholith.

The sample of quartz-feldspar rhyodacite porphyry from subcrop in the study area (sample MA11-001BV) gives an age of 57.2±1.0 Ma (latest Paleocene), which is similar to ages obtained for felsic dykes and plugs throughout the Dawson Range and areas to the north (Mortensen, unpublished data).

$^{40}Ar/^{39}Ar$ GEOCHRONOLOGY

SAMPLE AND METHODOLOGY

$^{40}Ar/^{39}Ar$ geochronology was used to determine the age of a sample of hydrothermal sericite from a quartz-carbonate-stibnite-gold vein with a strong sericite selvage (sample BV23_70.37m from diamond drill core). The hydrothermal sericite is interpreted to have formed at the same time as gold and stibnite mineralization.

Sericite grains were hand-picked from the sample under a binocular microscope, wrapped in aluminum foil, and stacked in an irradiation capsule with similar-aged samples and neutron flux monitors (Fish Canyon Tuff sanidine (FCS); 28.03 Ma (Renne *et al.*, 1998). The methodology used in this study for $^{40}Ar/^{39}Ar$ dating at PCIGR is similar to that described by Mortensen *et al.* (2010). The Boulevard sericite sample was irradiated from May 4 to 5, 2011 at the McMaster Nuclear Reactor in Hamilton, Ontario, for 45 MWH, with a neutron flux of approximately 6×10^{13} neutrons/cm^2/s. Analyses (n=45) of 15 neutron flux monitor positions produced errors of <0.5% in the J value. The sample was split into two separate aliquots after irradiation, and the samples were analysed from June through October 2011 at the Noble Gas Laboratory in the PCIGR.

RESULTS

The first aliquot of hydrothermal sericite yielded a plateau age of 95.9±0.9 Ma (MSWD=0.97, probability=0.41; plateau based on 74.3% of the ^{39}Ar; Fig. 13; Table 2). The duplicate analysis did not settle to enough steps to yield a plateau age, but the results are consistent with the age obtained from the first aliquot.

$^{187}Re/^{187}Os$ GEOCHRONOLOGY

SAMPLES AND METHODOLOGY

$^{187}Re/^{187}Os$ dating methods were utilized to constrain the age of molybdenite mineralization at the Toni Tiger showing. Two samples of molybdenite were dated: (a) a quartz-molybdenite vein crosscutting a meta-aplite (I034208); and (b) a quartz-molybdenite vein crosscutting garnet-actinolite-diopside skarn (I034229). Molybdenite in each sample occurs as coarse-grained rosettes mantled by vein quartz.

Samples were prepared and analysed by R. Creaser at the Radiogenic Isotope Laboratory at the University of Alberta according to the methods described by Selby and Creaser (2004) and Markey *et al.* (2007).

RESULTS

Analytical results for the two samples are given in Table 3. Sample I034208 yielded a Re-Os age of 95.0±0.4 Ma. Sample I034229 contains high common Os, hence the derived age is sensitive to assumed initial $^{187}Os/^{188}Os$ ratio. Assuming an initial $^{187}Os/^{188}Os$ value of 0.3, a somewhat younger age of 92.4±0.7 Ma is determined for this sample.

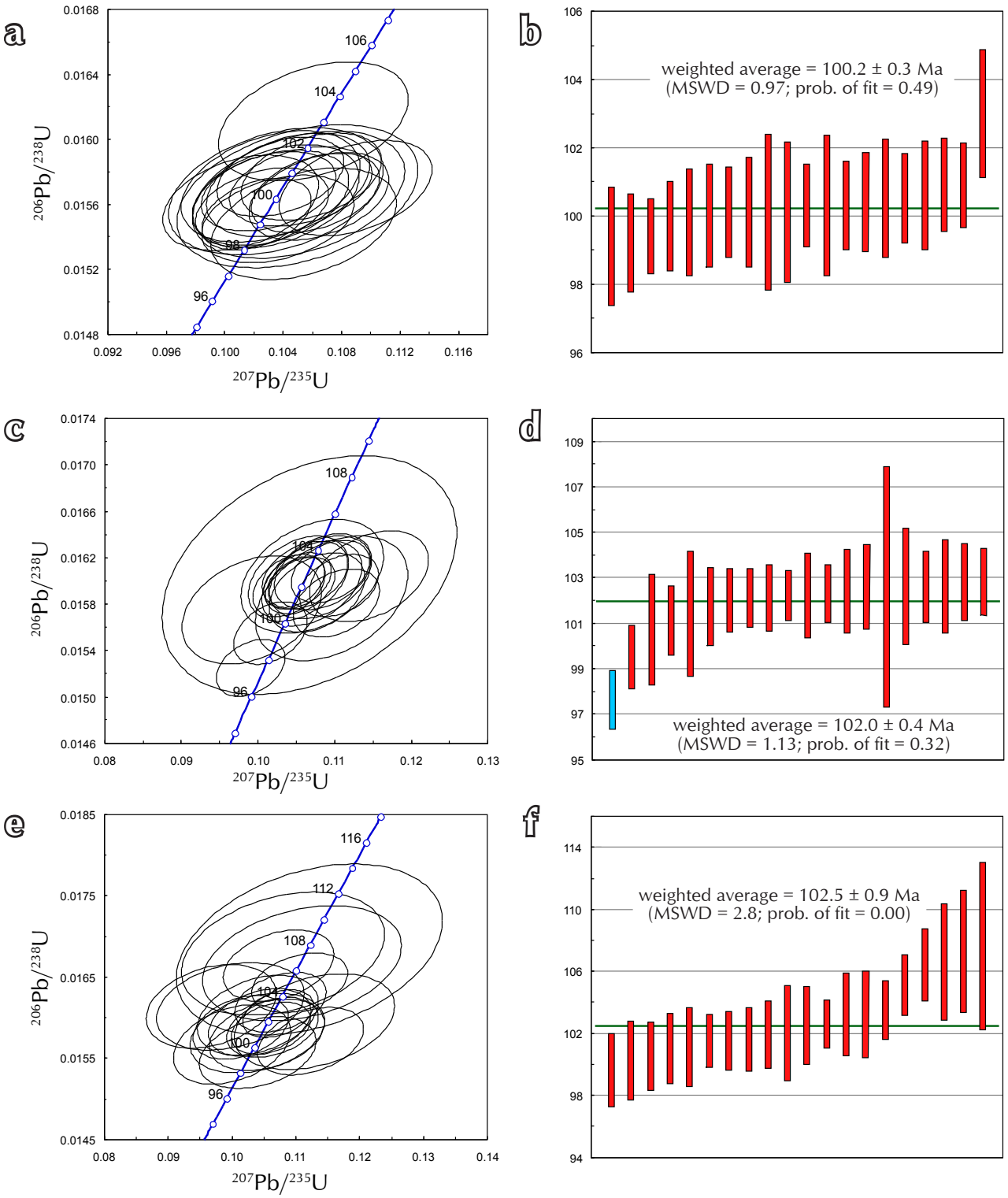

Figure 11. *Conventional concordia diagrams and plots of weighted average $^{206}Pb/^{238}U$ ages for samples of the Dawson Range batholith in the study area: (a) and (b) sample I034239 - biotite-hornblende granodiorite; (c) and (d) sample YGP-BV-004 - biotite-hornblende granodiorite; (e) and (f) sample 99M-106-b – aplite dyke cutting granodiorite. Symbols as in Figure 9.*

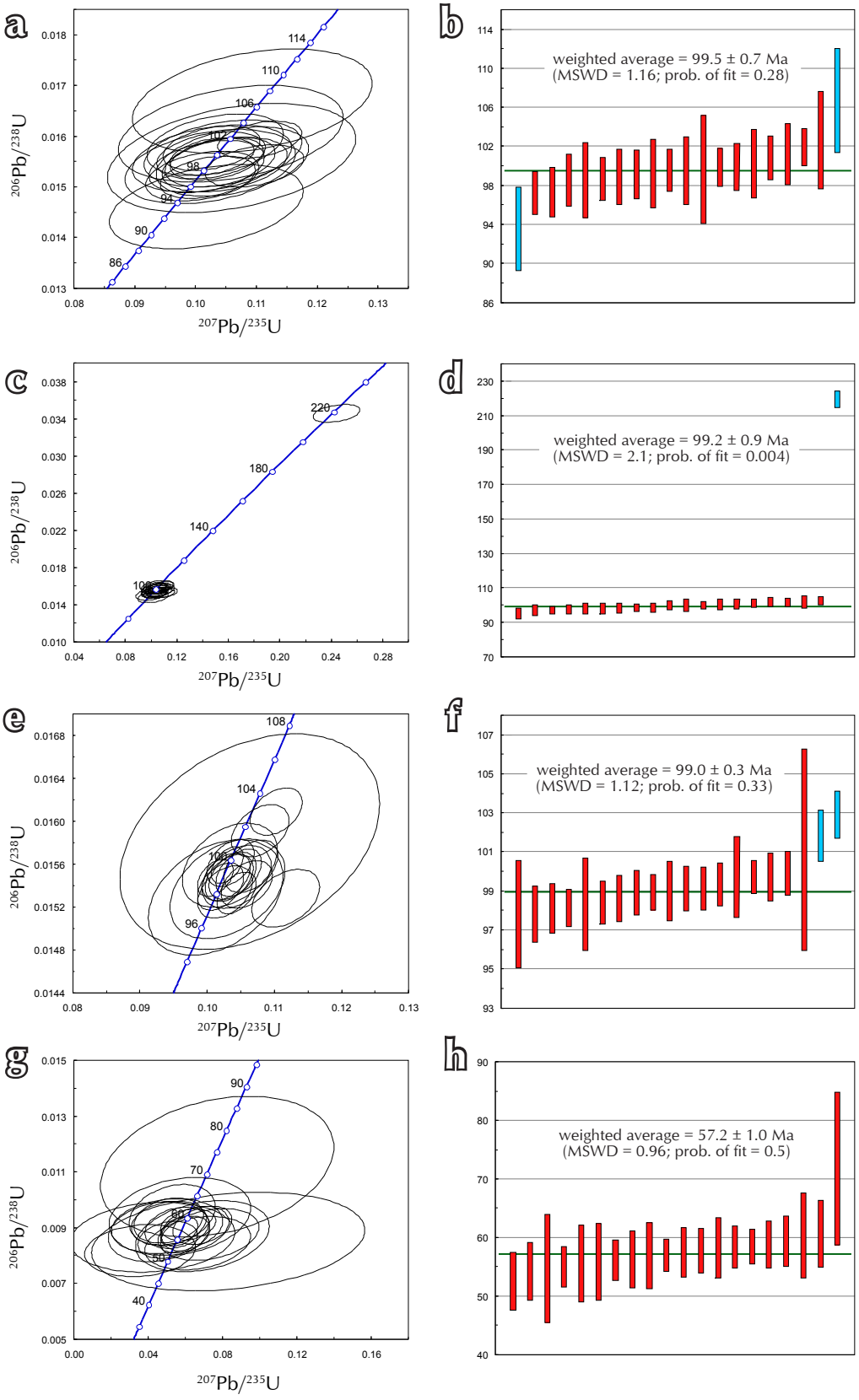

Figure 12. *Conventional concordia diagrams and plots of weighted average $^{206}Pb/^{238}U$ ages for samples of the Coffee Creek intrusions and a young subvolcanic rock in the study area: (a) and (b) sample YGR-BV-002 – biotite granite; (c) and (d) sample 99M-105 – biotite granite; (e) and (f) sample 99M-107 – biotite granite; (g) and (h) sample MA11-001BV - quartz-feldspar rhyodacite porphyry. Symbols as in Figure 9.*

Table 1. *$^{206}Pb/^{238}U$ zircon ages for Independence Creek samples.*

Sample	Rock Description	Unit	Location (NAD83 UTM zone 7N)		Age (Ma)	±2σ
			Easting	Northing		
METAMORPHIC ROCKS						
I034207	meta-aplite*	Klondike assemblage	577980	6966729	251.3	1.3
I034224	felsic orthogneiss*	Klondike assemblage	578139	6966731	255.2	0.6
GM11-9b	quartz-feldspar-biotite schist	Klondike assemblage	572444	6980691	249.6	4.4
MA11-004BV	quartz-feldspar-biotite schist	Klondike assemblage	563229	6972572	267.2	5.9
MA11-005BV	quartz-feldspar-biotite schist	Klondike assemblage	561996	6976060	260.6	5.4
MA11-006BV	quartz-feldspar-biotite schist	Klondike assemblage	561398	6975930	257.6	4.9
PLUTONIC ROCKS						
I034239	biotite-hornblende granodiorite	Dawson Range batholith	574610	6963807	100.2	0.3
YGR-BV-004	biotite-hornblende granodiorite	Dawson Range batholith	566127	6967606	102.0	0.4
99M-106-b	aplite cutting granodiorite	Dawson Range batholith	566278	6961313	102.5	0.9
YGR-BV-002	biotite granite*	Coffee Creek granite	573497	6968539	99.5	0.7
99M-105	biotite granite	Coffee Creek granite	577775	6968097	99.2	0.9
99M-107	biotite granite	Coffee Creek granite	560386	6973241	99.0	0.3
SUBVOLCANIC ROCKS						
MA11-001BV	quartz-feldspar rhyodacite porphyry	Skukum volcanic suite	574845	6964377	57.2	1.0

*molybdenite observed in heavy mineral separates

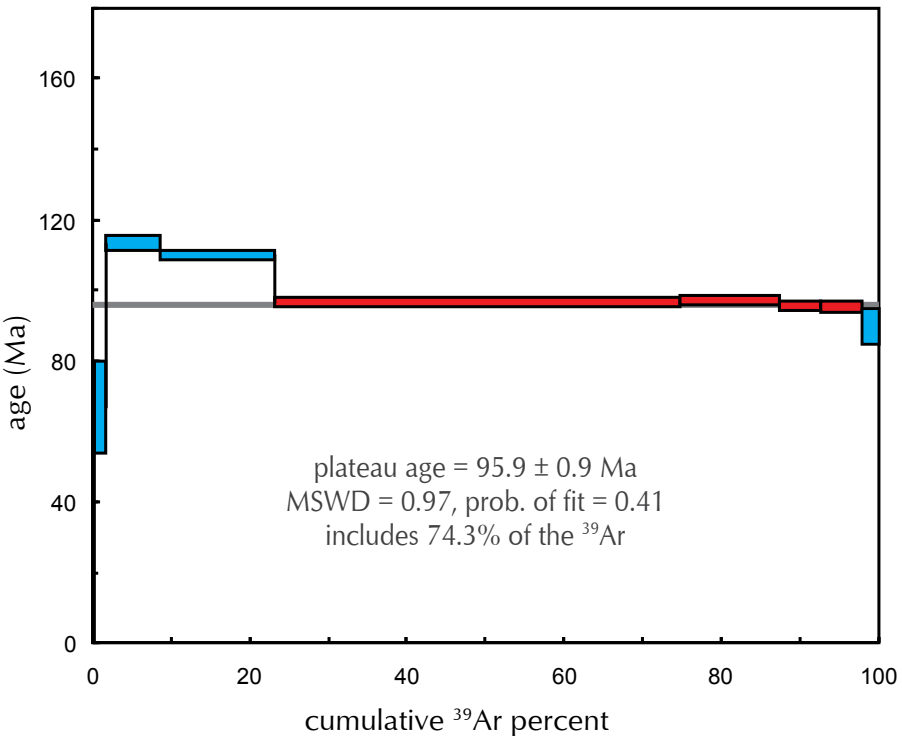

Figure 13. *Age spectra for step-heating of sericite sample BV23-70.37m from the Boulevard property. Error boxes and the calculated age are given at the 2σ level. Steps shown in red define the calculated plateau age; steps in blue were rejected.*

Table 2. *$^{40}Ar/^{39}Ar$ data for Boulevard sericite (Sample BV23_70.37m)*

	Isotope Ratios											
Laser power (%)	$^{40}Ar/^{39}Ar$	1σ	$^{37}Ar/^{39}Ar$	1σ	$^{36}Ar/^{39}Ar$	1σ	Ca/K	%^{40}Ar atm	f ^{39}Ar	$^{40}Ar^*/^{39}ArK$	Age	2σ
2.20 W	22.38	0.40	0.62	0.09	0.067	0.006	1.13	88.77	0.34	2.515	27.44	±39.95
2.60 W	24.21	0.22	0.07	0.03	0.061	0.002	0.12	74.58	1.54	6.154	66.43	±12.64
3.00 W	13.67	0.09	0.47	0.02	0.010	0.000	0.87	22.50	6.68	10.596	112.92	±2.08
3.50 W	10.72	0.07	0.28	0.01	0.002	0.000	0.52	4.35	14.70	10.259	109.44	±1.43
4.00 W	9.20	0.06	0.01	0.00	0.001	0.000	0.02	2.27	51.34	8.987	96.21	±1.17
4.40 W	9.26	0.06	0.01	0.00	0.001	0.000	0.02	2.69	12.50	9.014	96.50	±1.23
5.00 W	9.70	0.06	0.02	0.01	0.003	0.000	0.04	8.38	5.12	8.891	95.22	±1.59
6.00 W	10.11	0.06	0.06	0.01	0.004	0.000	0.10	12.15	5.39	8.883	95.13	±1.61
7.00 W	13.01	0.14	0.02	0.02	0.016	0.001	0.03	35.99	2.39	8.330	89.36	±5.12
J = 0.0060810±0.0000304				Volume ^{39}ArK=0.378			Integrated Date = 99.34±0.58 Ma					
Plateau age=95.93±0.89 Ma (2σ, including J-error of 0.6%)				MSWD=0.97, probability=0.41			Includes 74.3% of the ^{39}Ar (steps 5 through 8)					
Inverse isochron (correlation age) results, plateau steps: Model 1 Solution (±95%-conf.) on 9 points							Age=98.4±7.6 Ma					
Initial $^{40}Ar/^{36}Ar$ =350±170				MSWD=75, probability=0								

Table 3. *Re-Os data for Toni Tiger molybdenite samples.*

Sample	Re (ppm)	±2σ	^{187}Re (ppb)	±2σ	^{187}Os (ppb)	±2σ	Total common Os (pg)	Model Age (Ma)	±2σ
I034208	42.96	0.11	27002	71	42.76	0.04	1.6	95.0	0.4
I034208 (duplicate)	43.00	0.11	27029	70	42.76	0.04	1.6	94.9	0.4
I034228	27.62	0.08	17361	53	26.74	0.16	90.8	92.4	0.7

DISCUSSION

U-Pb GEOCHRONOLOGY

The 250 to 267 Ma age range of meta-igneous rocks in the Independence Creek area overlaps with that of the Late Permian Klondike volcanic arc assemblage and intrusive equivalents (Sulphur Creek orthogneiss) elsewhere in western Yukon (Mortensen, 1990; Ruks *et al.*, 2006; Beranek and Mortensen, 2011). We therefore concur with recent mapping by the Geological Survey of Canada which demonstrates that exposures of Klondike arc rocks in the Ladue River area (NTS 115N) continue eastward along the northern margin of the Dawson Range batholith into the Stevenson Ridge map sheet (NTS 115J) (Ryan *et al.*, in prep.).

The mid-Cretaceous crystallization ages determined for the Dawson Range batholith (*ca.* 100 to 103 Ma) are consistent with current geochronological compilations (Breitspreicher and Mortensen, 2004). The slightly younger 99 to 100 Ma zircon ages for the Coffee Creek granite are consistent with the interpretation of Templeman-Kluit and Wanless (1975) that this unit is a slightly younger intrusive phase of the Whitehorse plutonic suite.

Subvolcanic rocks cutting the Dawson Range batholith were determined to be 57.2±1.0 Ma, and are therefore age-equivalent to the previously mapped Paleocene Skukum volcanic rocks 4 km to the south (Templeman-Kluit, 1974), and volcanic and subvolcanic rocks elsewhere in western Yukon (Breitsprecher and Mortensen, 2004).

TIMING OF MINERALIZATION

The 95.0 ± 0.4 Ma $^{187}Re/^{187}Os$ model age for molybdenite at Toni Tiger overlaps within 2σ error with the 95.9 ± 0.9 Ma $^{40}Ar/^{39}Ar$ cooling age for hydrothermal sericite at Boulevard. While the latter age could be interpreted as a minimum, there is sufficient geological evidence (*e.g.*, common structural style and fluid inclusion properties) that Boulevard and Toni Tiger are related hydrothermal systems. Therefore, we interpret the $^{187}Re/^{187}Os$ and $^{40}Ar/^{39}Ar$ methods as recording coeval mineralizing events at *ca.* 96-95 Ma. Importantly, the mineralization age post-dates crystallization of the Dawson Range batholith and Coffee Creek granite by 3-4 m.y. No younger phase of the Whitehorse plutonic suite has yet been recognized in the Independence Creek area (or anywhere else in western Yukon), nor do the field relationships suggest a magmatic role in mineralization. It is likely that heat and fluid flux related to the emplacement of the Dawson Range batholith and Coffee Creek plutonic suites were responsible for hornfelsing and skarnification in the vicinity of the Toni Tiger showing. However, the geochronologic results of this study suggest that Au-As-Sb-(Pb-Zn-Cu) and Mo mineralization record a distinct and younger event.

The low-salinity, aqueous-carbonic composition of fluids attending mineralization is consistent with orogenic fluids documented worldwide (Groves *et al.*, 2003). The association between gold and pyritic alteration halos to quartz-carbonate veins suggests that wall rock sulphidation is an important gold-precipitating mechanism. Depressurization associated with faulting and brecciation may also play an important role in destabilizing gold-bisulphide complexes (*e.g.*, Wilkinson and Johnston, 1996).

Molybdenite is not commonly reported in orogenic systems; however, the geochronological and fluid inclusion evidence suggests that Toni Tiger is part of the same post-magmatic orogenic system as Boulevard. The association of molybdenite with moderate temperature, moderate pressure, dilute aqueous-carbonic fluids implies that molybdenite transport occurs in nature at *P-T-X* conditions quite dissimilar to those encountered in high-temperature, low-pressure systems such as porphyry Mo deposits. We speculate that molybdenite may have been remobilized from the felsic metaplutonic host rocks, which locally contain significant background concentrations of molybdenite.

REGIONAL SIGNIFICANCE

This study contributes to the metallogenic framework of the Dawson Range, and may be relevant to other structurally-hosted gold prospects, such as the Coffee gold deposit northeast of the Independence Creek drainage (Kaminak Gold Corp.), and gold in the Moosehorn Range (parts of NTS 115N and 115K; Fig. 1). Mineralization in the Coffee area occurs within a series of structural corridors that cut all rock units, including the mid-Cretaceous Coffee Creek granite (Wainwright *et al.*, 2011). A common, *ca.* 96-95 Ma metallogenesis for gold mineralization at Boulevard and Coffee is permissible given field relationships, although Coffee is dominated by brittle (shallow?) features, whereas vein swarms at Boulevard more likely represent deeper crustal levels. In the case of the Moosehorn Range, mineralization has been dated by $^{40}Ar/^{39}Ar$ methods to 93-92 Ma, which post-dates the main phase of the magmatism by ~8 m.y. (Joyce, 2002). Fluid inclusions associated with the Moosehorn veins also overlap strongly in composition and trapping conditions with those at Boulevard. On the basis of currently available geochronological data and geological relationships, we propose a general model in which exhumation of the Dawson Range shortly after cessation of arc magmatism in mid-Cretaceous time was accompanied by brittle deformation, fluid flow, and mineralization. However, the tectonic and structural setting of the Dawson Range at this time is still not completely understood.

ACKNOWLEDGEMENTS

This study is part of GGM's MSc project, which was a component of the Yukon Gold Project, a collaborative research venture between the Mineral Deposit Research Unit (UBC) and a consortium of industry participants, including Aldrin Resource Corp., Barrick Gold Corp., Full Metal Minerals Corp., Gold Fields Canada Exploration, Northern Freegold Resources Ltd., Kinross Gold Corp., Radius Gold Inc., Silver Quest Resources Ltd., Taku Gold Corp., Teck Resources Ltd., and Underworld Resources Inc. The Natural Science and Engineering Research Council of Canada (NSERC) also provided matching funds for the industry contribution. We are grateful for the logistical, financial, scientific, and editorial contributions of Silver Quest Resources (now Independence Gold Corp.) and Equity Exploration Ltd., and in particular Kendra Johnston, Darcy Baker, Dave Pawliuk, Randy Turner, and Ryan Congdon. Jim Ryan of the Geological Survey of Canada is thanked for his thoughtful review and his contributions to the geological understanding of the Dawson Range.

REFERENCES

Allan, M.M., Morrison, G.W., and Yardley, B.W.D., 2011. Physicochemical evolution of a porphyry-breccia system: a laser ablation ICP-MS study of fluid inclusions in the Mount Leyshon Au deposit, Queensland, Australia. Economic Geology, vol. 106, no. 3, p. 413-436.

Beranek, L.P. and Mortensen, J.K., 2011. The timing and provenance record of the Late Permian Klondike orogeny in northwestern Canada and arc-continent collision along western North America. Tectonics, vol. 30, no. 5, p. TC5017.

Berman, R.G., Ryan, J.J., Gordey, S.P., and Villeneuve, M., 2007. Permian to Cretaceous polymetamorphic evolution of the Stewart River region, Yukon-Tanana Terrane, Yukon, Canada; P-T evolution linked with in situ SHRIMP monazite geochronology. Journal of Metamorphic Geology, vol. 25, p. 803-827.

Breitsprecher, K. and Mortensen, J.K. (comps.), 2004. YukonAge 2004: A database of isotopic age determinations for rock units from Yukon Territory. Yukon Geological Survey, CD-ROM.

Craig, D.B., 1970. Toni Tiger report: Soil and rock sampling, bulldozer trenching. Yukon mining assessment report number 060249.

Chartier, D., Couture, J.-F., Sim., R., and Starkey, J., 2013. Mineral resource evaluation, Coffee gold project, Yukon, Canada: Vancouver, Kaminak Gold Corp., 203 p. <http://kaminak.com/projects/sections_and_maps/reports/technical_report/> [accessed February 10, 2013]

Gordey, S.P. and Makepeace, A.J. (comps.), 2003. Yukon Digital Geology. Geological Survey of Canada, Open File 1749 and Yukon Geological Survey, Open File 2003-9(D).

Gordey, S.P. and Ryan, J.J., 2005. Geology, Stewart River area (115N, 115O and part of 115J), Yukon Territory. Geological Survey of Canada, Open File 4970, scale 1:250 000.

Groves, D.I., Goldfarb, R.J., Robert, F., and Hart, C.J.R., 2003. Gold deposits in metamorphic belts: Overview of current understanding, outstanding problems, future research, and exploration significance. Economic Geology, vol. 98, p. 1-29.

Jilson, G., 2000. Geochemical and geological report on the Dan, Man and Indy claims. Yukon mining assessment report number 094174.

Joyce, N.L., 2002. Geologic setting, nature, and structural evolution of intrusion-hosted Au-bearing quartz veins at the Longline occurrence, Moosehorn Range Area, west-central Yukon Territory. Unpublished MSc Thesis, University of British Columbia, Vancouver, 201 p.

MacKenzie, D., Craw, D., and Mortensen, J.K., 2008a. Structural controls on orogenic gold mineralisation in the Klondike goldfield, Canada. Mineralium Deposita, vol. 43, p. 435-448.

MacKenzie, D., Craw, D., and Mortensen J.K., 2008b. Thrust slices and associated deformation in the Klondike goldfields, Yukon. *In:* Yukon Exploration and Geology 2007, D.S. Emond, L.R. Blackburn, R.P. Hill and L.H. Weston (eds.), Yukon Geological Survey, p. 199-213.

MacKenzie, D. and Craw, D., 2012. Contrasting structural settings of mafic and ultramafic rocks in the Yukon-Tanana terrane. *In:* Yukon Exploration and Geology 2011, K.E. MacFarlane and P.J. Sack (eds.), Yukon Geological Survey, p. 115-127.

Markey, R., Stein, H.J., Hannah, J.L., Zimmerman, A., Selby, D. and Creaser, R.A., 2007. Standardizing Re–Os geochronology: A new molybdenite Reference Material (Henderson, USA) and the stoichiometry of Os salts. Chemical Geology, vol. 244, p. 74-87.

Mortensen, J.K., 1990. Geology and U - Pb geochronology of the Klondike District, west - central Yukon Territory. Canadian Journal of Earth Sciences, vol. 27, p. 903–914.

Mortensen, J.K., Craw, D., MacKenzie, D.J., Gabites, J.E., and Ullrich, T., 2010. Age and origin of orogenic gold mineralization in the Otago Schist Belt, South Island, New Zealand: Constraints from lead isotope and $^{40}Ar/^{39}Ar$ dating studies. Economic Geology, vol. 105, p. 777-793.

Renne, P.R., Swisher, C.C., Deino, A.L., Karner, D.B., Owens, T.L., and DePaolo, D.J., 1998. Intercalibration of standards, absolute ages and uncertainties in $^{40}Ar/^{39}Ar$ dating. Chemical Geology, vol. 145, p. 117-152.

Ruks, T.W., Piercey, S.J., Ryan, J.J., Villeneuve, M.E., and Creaser, R.A., 2006. Mid- to late Paleozoic K-feldspar augen granitoids of the Yukon-Tanana terrane, Yukon, Canada: Implications for crustal growth and tectonic evolution of the northern Cordillera. Geological Society of America Bulletin, vol. 118, p. 1212-1231.

Selby, D. and Creaser, R.A., 2004. Macroscale NTIMS and microscale LA-MC-ICP-MS Re-Os isotopic analysis of molybdenite: Testing spatial restrictions for reliable Re-Os age determinations, and implications for the decoupling of Re and Os within molybdenite. Geochimica et Cosmochimica Acta, vol. 68, p. 3897-3908.

Tafti, R., Mortensen, J.K., Lang, J.R., Rebagliati, M., and Oliver, J.L., 2009. Jurassic U-Pb and Re-Os ages for the newly discovered Xietongmen Cu-Au porphyry district, Tibet, PRC: Implications for metallogenic epochs in the southern Gangdese belt. Economic Geology, vol. 104, p. 127-136.

Templeman-Kluit, D.J., 1974. Reconnaissance geology of Aishihik Lake, Snag and part of the Stewart River map areas, west-central Yukon Territory. Geological Survey of Canada, Paper 73-14, 93 p.

Tempelman-Kluit, D. and Wanless, R., 1975. Potassium-argon age determinations of metamorphic and plutonic rocks in the Yukon Crystalline Terrane. Canadian Journal of Earth Sciences, vol. 12, p. 1895-1909.

Wainwright, A.J., Simmons, A.T., Finnigan, C.S., Smith, T.R., and Carpenter, R.L., 2011. Geology of new gold discoveries in the Coffee Creek area, White Gold District, west-central Yukon. *In:* Yukon Exploration and Geology 2010, K.E. MacFarlane, L.H. Weston, and C. Relf (eds.), Yukon Geological Survey, p. 233-247.

Wilkinson, J.J. and Johnston, J.D., 1996. Pressure fluctuations, phase separation, and gold precipitation during seismic fracture propagation. Geology, vol. 24, p. 395-398.

Yukon MINFILE, 2010. Yukon MINFILE - A database of mineral occurrences. Yukon Geological Survey, <www.geology.gov.yk.ca/databases_gis.html> [accessed October 17, 2012].

Zagorevski, A., Ryan, J., Roots, C., and Hayward, N., 2012. Ultramafic rock occurrences in the Dawson Range and their implications for the crustal structure of Yukon-Tanana terrane, Yukon (parts of 115I, J and K), Geological Survey of Canada, Open File 7105, 1 sheet. doi:10.4095/290992.

APPENDIX 1: LA-ICP-MS data for U-Pb analysis of zircons

Fraction	Isotopic Ratios							Isotopic Ages						Background corrected mean counts per second at specified mass							
	$^{207}Pb/^{235}U$	% 1σ	$^{206}Pb/^{238}U$	% 1σ	rho	$^{207}Pb/^{206}Pb$	% 1σ	$^{207}Pb/^{235}U$	± 1σ	$^{206}Pb/^{238}U$	± 1σ	$^{207}Pb/^{206}Pb$	± 1σ	202	204	206	207	208	232	235	238
METAMORPHIC ROCKS																					
Meta-aplite; Toni Tiger (sample I034207)																					
1	0.22732	0.00829	0.03317	0.00043	0.36	0.05211	0.00181	208.0	6.9	210.3	2.7	290.2	77.5	0	13	11263	578	1826	84416	2267	475507
2	0.27569	0.00495	0.03830	0.00026	0.38	0.05298	0.00088	247.2	3.9	242.3	1.6	328.0	37.2	0	0	17138	894	3789	177690	2897	627073
3	0.24444	0.00658	0.03507	0.00034	0.36	0.05150	0.00131	222.0	5.4	222.2	2.1	263.4	57.2	48	0	13996	710	2508	114253	2597	559752
4	0.26753	0.01819	0.03905	0.00089	0.34	0.04842	0.00309	240.7	14.6	247.0	5.5	119.8	143.8	0	0	6711	320	1387	53669	1071	241284
5	0.28094	0.00659	0.03840	0.00033	0.37	0.05353	0.00117	251.4	5.2	242.9	2.1	351.3	48.8	46	19	26356	1391	5864	252194	4437	964482
6	0.28268	0.00636	0.03946	0.00032	0.36	0.05278	0.00110	252.8	5.0	249.5	2.0	319.2	46.5	0	11	16978	884	3336	164531	2808	605635
7	0.28513	0.01423	0.03959	0.00068	0.34	0.05182	0.00242	254.7	11.2	250.3	4.2	277.4	103.3	0	8	4223	216	618	29339	681	150316
8	0.25948	0.01319	0.03747	0.00066	0.35	0.05146	0.00247	234.2	10.6	237.1	4.1	261.5	106.4	0	0	5380	273	914	39886	948	202481
9	0.32504	0.01282	0.04000	0.00056	0.35	0.05560	0.00202	285.8	9.8	252.9	3.5	436.3	79.1	42	6	7064	388	1272	55999	1075	249223
10	0.27494	0.00542	0.03976	0.00029	0.37	0.05091	0.00092	246.6	4.3	251.4	1.8	236.8	41.1	13	0	43533	2190	9528	390740	7184	1546326
11	0.30709	0.01248	0.03991	0.00059	0.36	0.05736	0.00217	271.9	9.7	252.3	3.6	504.9	81.4	15	3	9286	526	1797	73673	1550	329174
12	0.28647	0.00600	0.03972	0.00030	0.36	0.05360	0.00102	255.8	4.7	251.1	1.9	354.0	42.7	3	0	16588	879	3450	164002	2778	591470
13	0.27896	0.00931	0.04000	0.00047	0.35	0.05084	0.00157	249.8	7.4	252.8	2.9	233.6	69.8	31	0	25811	1299	5207	239225	4217	914551
14	0.28211	0.00765	0.04013	0.00039	0.36	0.05188	0.00129	252.3	6.1	253.6	2.4	280.1	56.1	29	0	13773	707	2855	136341	2274	486898
15	0.29159	0.00975	0.03976	0.00047	0.35	0.05268	0.00163	259.8	7.7	251.3	2.9	314.8	68.7	0	6	13969	729	2550	117120	2269	498826
16	0.28043	0.00911	0.03985	0.00046	0.36	0.05221	0.00157	251.0	7.2	251.9	2.8	294.4	66.9	67	12	21147	1094	3089	142233	3550	754747
17	0.29249	0.00732	0.03980	0.00035	0.35	0.05165	0.00117	260.5	5.8	251.6	2.2	269.9	51.2	32	0	22110	1132	5287	241868	3526	790708
18	0.27207	0.01515	0.04006	0.00076	0.34	0.04904	0.00255	244.3	12.1	253.2	4.7	149.6	117.5	0	0	9587	466	1464	62744	1562	341000
19	0.28395	0.00717	0.03967	0.00036	0.36	0.05222	0.00119	253.8	5.7	250.8	2.2	295.1	51.3	0	13	14925	773	2626	124397	2486	536485
20	0.27796	0.00674	0.03959	0.00034	0.35	0.05184	0.00113	249.0	5.4	250.3	2.1	278.5	49.1	17	0	25914	1333	5760	262716	4384	934137
Orthogneiss with disseminated molybdenite (sample I034224)																					
1	0.27938	0.00948	0.03977	0.00047	0.35	0.05117	0.00162	250.2	7.5	251.4	2.9	248.7	71.3	0	17	1927	105	270	10809	396	59986
2	0.28927	0.00285	0.04021	0.00016	0.40	0.05245	0.00048	258.0	2.3	254.2	1.0	305.0	20.8	79	19	20294	1036	1451	49729	3185	488565
3	0.29348	0.00429	0.04066	0.00022	0.37	0.05340	0.00073	261.3	3.4	256.9	1.4	345.6	30.4	16	15	58321	3051	5208	157670	9064	1388549
4	0.29281	0.00518	0.04035	0.00026	0.36	0.05127	0.00084	260.8	4.1	255.0	1.6	253.1	37.3	21	0	31217	1662	2645	81968	4869	734983
5	0.30010	0.00450	0.04034	0.00022	0.36	0.05264	0.00073	266.5	3.5	254.9	1.4	313.3	31.3	24	18	28110	1437	1810	58298	4221	666974
6	0.28341	0.00501	0.04075	0.00026	0.36	0.05049	0.00083	253.4	4.0	257.5	1.6	217.6	37.7	0	32	43875	2370	1536	36805	5034	777004
7	0.28258	0.00353	0.04025	0.00019	0.38	0.05061	0.00059	252.7	2.8	254.4	1.2	223.1	26.7	11	14	28187	1419	2073	68133	4308	662094
8	0.29118	0.00458	0.04029	0.00023	0.36	0.05271	0.00077	259.5	3.6	254.6	1.4	316.2	32.9	76	0	23488	1185	1587	49293	3610	558547
9	0.28938	0.00614	0.04025	0.00030	0.35	0.05150	0.00102	258.1	4.8	254.4	1.9	263.4	44.8	0	6	26627	1399	2116	66524	4137	632458
10	0.28675	0.00391	0.04057	0.00020	0.36	0.05140	0.00065	256.0	3.1	256.3	1.3	258.6	29.0	28	0	10377	532	740	25012	1585	246735
11	0.28576	0.00333	0.04043	0.00018	0.38	0.05193	0.00056	255.2	2.6	255.5	1.1	282.1	24.7	0	13	52149	2800	1735	40924	6054	929877
12	0.27521	0.00424	0.04048	0.00023	0.37	0.05056	0.00073	246.9	3.4	255.8	1.4	220.9	32.9	12	15	40033	2071	3886	124505	6249	947227
13	0.28684	0.00379	0.04077	0.00020	0.37	0.05012	0.00061	256.1	3.0	257.6	1.2	200.8	28.2	29	5	45555	2295	3490	112200	7192	1076595
14	0.28447	0.00556	0.04041	0.00028	0.35	0.05062	0.00092	254.2	4.4	255.4	1.7	223.6	41.6	43	2	29842	1490	1928	65001	4482	700193
15	0.28312	0.00664	0.04014	0.00033	0.35	0.05081	0.00111	253.1	5.3	253.7	2.1	232.0	49.7	17	15	25043	1262	2582	78531	3831	592793
16	0.29153	0.00305	0.04031	0.00016	0.38	0.05340	0.00052	259.8	2.4	254.7	1.0	345.9	21.8	0	40	73133	3808	2400	57873	8370	1291864
17	0.28605	0.00500	0.04059	0.00026	0.37	0.05225	0.00085	255.4	4.0	256.5	1.6	296.4	36.8	13	0	44902	2388	4934	145861	7075	1065334
18	0.29158	0.00633	0.04021	0.00031	0.36	0.05217	0.00105	259.8	5.0	254.1	1.9	292.7	45.5	29	0	17089	889	1773	54829	2685	402584
19	0.28156	0.00701	0.03976	0.00035	0.35	0.05132	0.00119	251.9	5.6	251.3	2.2	255.2	52.6	59	0	11604	602	897	29368	1786	275968
20	0.29416	0.00424	0.04030	0.00021	0.36	0.05251	0.00070	261.8	3.3	254.7	1.3	307.5	30.2	8	0	11765	601	905	29190	1845	282946
Quartz-feldspar-biotite schist (sample GM11-9b)																					
1	0.25657	0.01470	0.03673	0.00084	0.40	0.04957	0.00273	231.9	11.9	232.5	5.2	175.0	123.6	0	0	3079	153	733	41387	542	119334
2	0.29233	0.00763	0.03905	0.00064	0.63	0.05195	0.00131	260.4	6.0	246.9	4.0	283.2	56.4	0	0	7907	413	1103	53709	1283	288676
3	0.28847	0.01147	0.04132	0.00078	0.47	0.05003	0.00189	257.4	9.0	261.0	4.8	196.5	85.7	0	0	5523	277	737	38125	875	190838
4	0.27832	0.00729	0.03932	0.00064	0.62	0.05129	0.00130	249.3	5.8	248.6	4.0	253.9	57.5	0	0	6710	346	1007	46838	1131	243938
5	0.27585	0.00878	0.03894	0.00069	0.56	0.05080	0.00155	247.4	7.0	246.2	4.3	231.9	68.9	30	0	8674	442	1383	66059	1466	320218
6	0.28040	0.00992	0.03907	0.00072	0.52	0.05440	0.00185	251.0	7.9	247.0	4.5	387.7	73.9	64	37	6024	329	1068	52052	1073	221963
7	0.28050	0.00727	0.03989	0.00066	0.64	0.05082	0.00127	251.1	5.8	252.1	4.1	232.7	56.6	0	0	10915	557	1644	86173	1818	394440
8	0.29362	0.01197	0.03921	0.00075	0.47	0.05180	0.00202	261.4	9.4	247.9	4.6	276.7	86.9	0	16	4022	209	382	18062	652	148050
Quartz-feldspar-biotite schist (sample MA11-004BV)																					
1	0.30444	0.00933	0.04065	0.00074	0.59	0.05233	0.00152	269.9	7.3	256.8	4.6	299.8	64.7	14	0	7901	419	1187	49235	1287	296695
2	0.28924	0.00731	0.04175	0.00071	0.67	0.04956	0.00119	258.0	5.8	263.7	4.4	174.6	55.3	0	0	9084	456	1323	60316	1475	331715
3	0.29287	0.01080	0.04190	0.00080	0.52	0.05170	0.00182	260.8	8.5	264.6	5.0	272.3	78.6	43	0	4293	225	608	29029	718	156037
4	0.29939	0.01202	0.04269	0.00084	0.49	0.05247	0.00201	265.9	9.4	269.5	5.2	305.8	84.8	0	8	3209	170	402	16357	533	114527
5	0.31044	0.00937	0.04286	0.00077	0.60	0.05181	0.00148	274.5	7.3	270.5	4.8	276.8	64.1	48	0	6435	338	950	46785	1018	229090

APPENDIX 1 (continued): LA-ICP-MS data for U-Pb analysis of zircons

Fraction	Isotopic Ratios							Isotopic Ages						Background corrected mean counts per second at specified mass							
	$^{207}Pb/^{235}U$	% 1σ	$^{206}Pb/^{238}U$	% 1σ	rho	$^{207}Pb/^{206}Pb$	% 1σ	$^{207}Pb/^{235}U$	± 1σ	$^{206}Pb/^{238}U$	± 1σ	$^{207}Pb/^{206}Pb$	± 1σ	202	204	206	207	208	232	235	238
6	0.28127	0.01061	0.04327	0.00084	0.51	0.04796	0.00172	251.7	8.4	273.1	5.2	96.1	83.7	30	0	7838	381	850	41679	1267	276207
7	0.28356	0.00909	0.04354	0.00079	0.57	0.04854	0.00148	253.5	7.2	274.7	4.9	125.7	70.4	0	0	4986	245	687	34454	809	174536
Quartz-feldspar-biotite schist (sample MA11-00BV)																					
1	0.27302	0.01502	0.03903	0.00071	0.33	0.04866	0.00254	245.1	12.0	246.8	4.4	131.5	118.4	10	0	5428	270	1105	62508	940	211402
2	0.26837	0.00877	0.04095	0.00044	0.33	0.04909	0.00153	241.4	7.0	258.7	2.7	151.9	71.5	72	0	5311	266	900	46700	944	197212
3	0.29940	0.00657	0.04370	0.00034	0.35	0.04979	0.00102	265.9	5.1	275.7	2.1	185.1	47.0	0	0	16053	816	3773	192569	2596	558601
4	0.27581	0.00996	0.04346	0.00049	0.31	0.04858	0.00167	247.3	7.9	274.3	3.1	127.6	79.2	0	0	4741	235	709	32801	812	165891
5	0.29195	0.00965	0.04187	0.00047	0.34	0.05138	0.00161	260.1	7.6	264.4	2.9	257.7	70.2	29	0	6807	356	1568	74478	1165	247295
6	0.26983	0.01171	0.04185	0.00059	0.32	0.04776	0.00197	242.6	9.4	264.3	3.7	86.2	96.0	0	16	5966	290	1128	57105	1027	216958
7	0.26631	0.02535	0.04179	0.00098	0.25	0.04461	0.00414	239.7	20.3	263.9	6.0	0.1	135.3	10	1	1174	53	146	6759	191	42770
8	0.28989	0.00957	0.04241	0.00047	0.34	0.04947	0.00154	258.5	7.5	267.7	2.9	170.0	71.0	0	30	9214	464	2131	113157	1530	330789
9	0.27844	0.01648	0.03946	0.00072	0.31	0.05054	0.00287	249.4	13.1	249.5	4.5	220.0	126.2	0	9	2708	139	592	32543	478	104528
10	0.29632	0.01099	0.04209	0.00051	0.33	0.05297	0.00187	263.5	8.6	265.8	3.2	327.3	78.2	40	0	4220	227	775	40736	734	152722
11	0.27940	0.01856	0.04055	0.00073	0.27	0.05321	0.00345	250.2	14.7	256.3	4.5	337.8	139.8	0	15	1514	81	268	15229	280	56894
12	0.27109	0.01013	0.04071	0.00048	0.32	0.04867	0.00173	243.6	8.1	257.2	3.0	132.1	81.7	0	0	4395	217	651	30191	768	164560
13	0.27030	0.01532	0.03812	0.00075	0.35	0.05249	0.00284	242.9	12.3	241.2	4.7	307.0	118.4	53	0	5329	284	861	41672	1007	213132
14	0.30912	0.01071	0.03938	0.00045	0.33	0.05406	0.00178	273.5	8.3	249.0	2.8	373.5	72.1	10	0	4298	235	847	40381	731	166449
15	0.29082	0.00810	0.04144	0.00039	0.34	0.05104	0.00134	259.2	6.4	261.8	2.4	242.7	59.4	31	20	7698	398	1354	71808	1315	283362
16	0.31232	0.03578	0.04052	0.00127	0.27	0.05512	0.00614	276.0	27.7	256.1	7.9	416.8	231.6	6	2	791	44	123	7043	135	29792
17	0.30215	0.02702	0.03992	0.00119	0.33	0.05659	0.00485	268.1	21.1	252.4	7.4	474.8	179.8	16	0	1687	96	171	10462	307	64522
18	0.29176	0.00974	0.03816	0.00044	0.35	0.05261	0.00166	259.9	7.7	241.4	2.7	312.1	70.0	41	19	8325	443	1254	60535	1462	333064
Quartz-feldspar-biotite schist (sample MA11-006BV)																					
1	0.29397	0.02112	0.04087	0.00079	0.27	0.04900	0.00340	261.7	16.6	258.3	4.9	147.9	155.2	48	22	1394	70	86	4280	225	51587
2	0.37578	0.08776	0.04096	0.00295	0.31	0.06069	0.01352	323.9	64.8	258.8	18.3	628.2	418.9	31	0	634	39	18	1260	99	23428
3	0.21468	0.04316	0.04390	0.00219	0.25	0.04152	0.00817	197.5	36.1	276.9	13.5	0.1	180.6	0	11	1039	44	87	2468	195	35823
4	0.30923	0.02692	0.04150	0.00122	0.34	0.05442	0.00449	273.6	20.9	262.1	7.6	388.4	175.4	94	5	2847	160	252	10733	486	103785
5	0.27573	0.01454	0.04088	0.00062	0.29	0.04785	0.00243	247.3	11.6	258.3	3.9	90.9	117.1	0	8	2428	120	142	4879	409	89877
6	0.22786	0.05184	0.04770	0.00225	0.21	0.03468	0.00770	208.4	42.9	300.4	13.9	0.1	0.0	67	32	927	33	50	1939	137	29422
7	0.27361	0.04224	0.03854	0.00192	0.32	0.05754	0.00862	245.6	33.7	243.8	11.9	511.8	299.6	0	0	1148	68	30	1149	234	45096
8	0.29634	0.01954	0.04320	0.00089	0.31	0.05489	0.00348	263.5	15.3	272.6	5.5	407.8	135.9	0	5	1877	106	173	5424	337	65816
9	0.27598	0.02158	0.03874	0.00106	0.35	0.05634	0.00423	247.5	17.2	245.0	6.6	465.1	159.0	0	17	2970	172	232	5826	588	116121
10	0.22468	0.05914	0.03649	0.00257	0.27	0.04864	0.01257	205.8	49.0	231.0	16.0	130.5	516.1	0	23	807	40	61	4437	169	33507
11	0.16223	0.04266	0.03988	0.00200	0.19	0.03089	0.00802	152.6	37.3	252.1	12.4	0.1	0.0	0	0	905	28	60	1568	167	34402
12	0.22684	0.11359	0.04484	0.00485	0.22	0.04176	0.02057	207.6	94.0	282.8	29.9	0.1	685.5	0	31	406	17	0	1138	72	13726
13	0.28429	0.02248	0.04037	0.00096	0.30	0.04928	0.00374	254.1	17.8	255.1	5.9	161.0	168.4	0	0	1646	83	89	3255	277	61816
14	0.31003	0.04637	0.04282	0.00206	0.32	0.05553	0.00794	274.2	35.9	270.3	12.7	433.2	290.6	49	22	1162	66	45	3492	202	41150
15	0.34142	0.03704	0.03751	0.00152	0.37	0.07186	0.00748	298.3	28.0	237.4	9.4	981.8	198.6	60	0	1561	115	104	6742	319	63137
16	0.26982	0.02803	0.03911	0.00109	0.27	0.04637	0.00466	242.6	22.4	247.3	6.8	16.7	225.5	42	3	1344	63	52	3658	224	52148
17	0.28383	0.02723	0.04190	0.00125	0.31	0.05187	0.00478	253.7	21.5	264.6	7.8	279.9	197.6	0	19	1538	81	83	4189	273	55749
18	0.23190	0.04571	0.04261	0.00181	0.22	0.03718	0.00716	211.8	37.7	269.0	11.2	0.1	0.0	0	0	873	33	77	1843	136	31120
19	0.28504	0.05041	0.04050	0.00196	0.27	0.05263	0.00905	254.6	39.8	255.9	12.2	312.9	350.3	0	0	778	42	47	2667	139	29202
PLUTONIC ROCKS																					
Dawson Range batholith (sample I034239)																					
1	0.10313	0.00219	0.01564	0.00012	0.36	0.04754	0.00101	99.7	2.0	100.0	0.8	75.6	50.5	13	0	11060	552	1631	67944	2216	340250
2	0.10592	0.00196	0.01577	0.00011	0.38	0.04813	0.00089	102.2	1.8	100.9	0.7	105.5	43.2	19	19	8601	406	621	52022	3417	525794
3	0.10620	0.00179	0.01567	0.00010	0.38	0.04850	0.00082	102.5	1.7	100.3	0.6	123.5	39.3	14	2	15138	724	1629	129999	5929	917171
4	0.10254	0.00186	0.01558	0.00010	0.35	0.04795	0.00087	99.1	1.7	99.7	0.7	95.8	43.6	1	6	11681	563	1461	116562	4599	712199
5	0.10218	0.00153	0.01554	0.00009	0.39	0.04795	0.00072	98.8	1.4	99.4	0.6	95.6	36.2	0	0	12086	576	1404	116038	4874	741201
6	0.10434	0.00228	0.01572	0.00013	0.38	0.04865	0.00107	100.8	2.1	100.6	0.8	131.2	50.8	27	0	35287	1856	913	23298	4109	625473
7	0.10313	0.00250	0.01571	0.00014	0.37	0.04807	0.00117	99.7	2.3	100.5	0.9	102.6	56.7	8	35	13151	636	1661	149217	5292	799216
8	0.10644	0.00195	0.01565	0.00011	0.38	0.04958	0.00091	102.7	1.8	100.1	0.7	175.3	42.1	35	31	9257	442	1107	96917	3724	563091
9	0.10351	0.00232	0.01565	0.00013	0.37	0.04824	0.00108	100.0	2.1	100.1	0.8	110.9	52.2	29	0	14203	700	1609	129950	5711	867021
10	0.10109	0.00218	0.01561	0.00012	0.36	0.04731	0.00102	97.8	2.0	99.8	0.8	64.2	51.3	24	3	18249	875	2904	222778	7343	1113660
11	0.10497	0.00337	0.01565	0.00018	0.36	0.04905	0.00158	101.4	3.1	100.1	1.1	150.3	74.0	44	1	20874	1102	523	14160	2398	372224
12	0.10606	0.00265	0.01611	0.00015	0.37	0.04909	0.00123	102.4	2.4	103.0	0.9	152.3	57.8	50	15	4481	218	439	39207	1809	273493
13	0.10540	0.00259	0.01548	0.00014	0.37	0.04897	0.00121	101.7	2.4	99.1	0.9	146.3	56.9	44	4	14555	710	2254	186289	5822	862807
14	0.10895	0.00214	0.01570	0.00012	0.39	0.05040	0.00099	105.0	2.0	100.4	0.7	213.6	44.9	15	33	6719	326	565	47232	2698	414314
15	0.10351	0.00300	0.01568	0.00016	0.35	0.04659	0.00136	100.0	2.8	100.3	1.0	27.9	67.4	7	5	14598	731	2015	164846	5839	887894
16	0.10382	0.00177	0.01577	0.00010	0.37	0.04726	0.00080	100.3	1.6	100.9	0.6	62.0	40.5	3	16	43022	2247	1343	36109	5061	765585

APPENDIX 1 (continued): LA-ICP-MS data for U-Pb analysis of zircons

Fraction	Isotopic Ratios							Isotopic Ages						Background corrected mean counts per second at specified mass							
	$^{207}Pb/^{235}U$	% 1σ	$^{206}Pb/^{238}U$	% 1σ	rho	$^{207}Pb/^{206}Pb$	% 1σ	$^{207}Pb/^{235}U$	± 1σ	$^{206}Pb/^{238}U$	± 1σ	$^{207}Pb/^{206}Pb$	± 1σ	202	204	206	207	208	232	235	238
17	0.10504	0.00297	0.01566	0.00016	0.36	0.04923	0.00140	101.4	2.7	100.1	1.0	158.9	65.2	11	0	13914	653	1554	127026	5480	842157
18	0.10520	0.00199	0.01571	0.00010	0.34	0.04793	0.00090	101.6	1.8	100.5	0.7	94.8	45.0	35	0	9197	449	945	79945	3730	560775
19	0.10363	0.00213	0.01551	0.00011	0.35	0.04764	0.00098	100.1	2.0	99.2	0.7	80.4	48.7	26	1	10141	482	1312	109430	3999	616125
20	0.10300	0.00188	0.01568	0.00010	0.35	0.04738	0.00086	99.5	1.7	100.3	0.7	67.6	43.2	0	19	9439	446	839	73189	3756	580982
Dawson Range batholith (sample YGR-BV-004)																					
1	0.10816	0.00271	0.01604	0.00015	0.37	0.04867	0.00123	104.3	2.5	102.6	0.9	131.9	58.3	47	33	5045	255	828	33112	989	161483
2	0.10517	0.00180	0.01600	0.00010	0.37	0.04730	0.00081	101.5	1.7	102.3	0.6	63.6	41.0	28	0	11730	571	922	75877	4498	701353
3	0.10500	0.00150	0.01599	0.00009	0.39	0.04812	0.00069	101.4	1.4	102.2	0.6	105.2	33.6	0	4	10464	494	1110	90678	4011	627331
4	0.10548	0.00186	0.01596	0.00010	0.36	0.04816	0.00085	101.8	1.7	102.1	0.7	107.4	41.4	0	19	28540	1373	3844	313351	11151	1712402
5	0.10702	0.00266	0.01598	0.00015	0.38	0.04885	0.00123	103.2	2.4	102.2	0.9	140.6	57.9	53	6	9717	468	1049	90530	3784	583817
6	0.10960	0.00406	0.01585	0.00022	0.37	0.04979	0.00186	105.6	3.7	101.4	1.4	185.3	84.8	60	15	50736	2690	1352	32020	5852	909921
7	0.11055	0.00212	0.01596	0.00011	0.36	0.04995	0.00097	106.5	1.9	102.1	0.7	192.8	44.4	42	0	11070	551	1108	84069	4291	669649
8	0.10164	0.00196	0.01555	0.00011	0.37	0.04757	0.00092	98.3	1.8	99.5	0.7	77.2	46.2	70	0	10103	504	859	66958	3896	606866
9	0.10529	0.00267	0.01602	0.00015	0.37	0.04724	0.00120	101.7	2.5	102.4	0.9	60.7	60.1	9	26	9814	466	960	81519	3920	605169
10	0.10671	0.00785	0.01605	0.00042	0.36	0.04770	0.00354	102.9	7.2	102.6	2.7	83.3	167.9	9	1	8261	390	802	61252	3164	494470
11	0.10708	0.00380	0.01604	0.00020	0.35	0.04677	0.00167	103.3	3.5	102.6	1.3	37.1	83.5	0	0	30432	1592	902	22842	3501	547028
12	0.10611	0.00228	0.01605	0.00012	0.35	0.04811	0.00104	102.4	2.1	102.6	0.8	104.6	50.3	7	0	10672	498	1067	86233	3982	637565
13	0.09918	0.00372	0.01575	0.00019	0.32	0.04671	0.00177	96.0	3.4	100.7	1.2	34.1	88.3	37	2	6585	316	610	49382	2551	393340
14	0.10404	0.00192	0.01596	0.00011	0.37	0.04772	0.00089	100.5	1.8	102.0	0.7	84.5	44.4	28	3	7845	366	528	42081	3157	477514
15	0.11022	0.00230	0.01581	0.00012	0.36	0.05038	0.00106	106.2	2.1	101.1	0.8	212.5	47.9	0	19	11944	569	769	63080	4683	717362
16	0.10769	0.00255	0.01590	0.00014	0.37	0.04775	0.00114	103.8	2.3	101.7	0.9	86.0	56.5	17	22	31449	1656	942	22387	3624	562180
17	0.10842	0.00257	0.01607	0.00013	0.34	0.04847	0.00116	104.5	2.4	102.8	0.8	122.1	55.3	16	24	7630	363	637	50748	2894	459903
18	0.10944	0.00210	0.01608	0.00011	0.36	0.04956	0.00096	105.5	1.9	102.8	0.7	174.5	44.3	0	0	5790	280	579	45829	2214	345148
19	0.11449	0.00316	0.01604	0.00016	0.36	0.05032	0.00140	110.1	2.9	102.6	1.0	209.8	63.2	65	12	13560	670	588	48007	5255	807922
20	0.09905	0.00182	0.01525	0.00010	0.36	0.04724	0.00087	95.9	1.7	97.6	0.7	60.7	43.9	0	14	6680	335	754	61826	2513	399033
Dawson Range batholith (sample 99M-106-b)																					
1	0.10799	0.00650	0.01679	0.00031	0.31	0.04620	0.00282	104.1	6.0	107.3	2.0	8.3	140.8	78	11	2679	124	271	27505	1336	199982
2	0.11228	0.00339	0.01571	0.00017	0.36	0.05142	0.00158	108.0	3.1	100.5	1.1	259.7	69.2	140	11	7967	412	1032	115385	4255	636020
3	0.10761	0.00293	0.01619	0.00015	0.34	0.04831	0.00133	103.8	2.7	103.5	1.0	114.3	63.8	90	14	5766	280	699	77492	3020	446698
4	0.10607	0.00254	0.01587	0.00013	0.34	0.04854	0.00118	102.4	2.3	101.5	0.9	125.5	56.2	135	25	7146	349	1324	158411	3817	565069
5	0.09674	0.00415	0.01614	0.00021	0.30	0.04363	0.00190	93.8	3.8	103.2	1.3	0.1	0.0	58	28	4303	189	573	68206	2268	334918
6	0.11060	0.00307	0.01643	0.00015	0.33	0.04825	0.00136	106.5	2.8	105.1	1.0	111.5	65.1	57	7	5408	262	664	76070	2758	413346
7	0.10403	0.00387	0.01603	0.00020	0.34	0.04758	0.00180	100.5	3.6	102.5	1.3	77.5	88.1	92	0	4179	200	536	66458	2236	327551
8	0.10402	0.00373	0.01557	0.00018	0.32	0.04918	0.00179	100.5	3.4	99.6	1.2	156.2	83.2	120	0	4379	217	757	83915	2423	353458
9	0.10636	0.00293	0.01588	0.00015	0.34	0.04808	0.00134	102.6	2.7	101.5	1.0	103.3	64.6	58	8	5301	256	755	85706	2808	420096
10	0.11290	0.00513	0.01595	0.00024	0.33	0.04981	0.00230	108.6	4.7	102.0	1.5	186.0	104.1	71	31	3888	195	488	57385	2011	306718
11	0.11096	0.00635	0.01667	0.00029	0.30	0.04864	0.00283	106.8	5.8	106.6	1.9	130.3	131.3	1	12	2134	104	220	24960	1097	161205
12	0.10729	0.00354	0.01664	0.00018	0.33	0.04719	0.00158	103.5	3.3	106.4	1.2	58.6	78.4	46	1	4184	199	592	61085	2160	316705
13	0.10720	0.00226	0.01605	0.00012	0.35	0.04806	0.00102	103.4	2.1	102.6	0.8	102.4	49.4	0	28	9342	452	2235	243214	4923	733931
14	0.09973	0.00472	0.01614	0.00022	0.29	0.04614	0.00221	96.5	4.4	103.2	1.4	5.1	111.5	59	12	2479	115	325	38244	1349	193759
15	0.10397	0.00431	0.01581	0.00020	0.31	0.04705	0.00198	100.4	4.0	101.1	1.3	51.3	97.6	22	0	3555	168	463	55385	1892	283647
16	0.10139	0.00305	0.01588	0.00016	0.33	0.04648	0.00142	98.1	2.8	101.6	1.0	22.4	70.6	98	21	5410	253	779	80935	2918	429910
17	0.10432	0.00328	0.01594	0.00017	0.34	0.04823	0.00154	100.8	3.0	101.9	1.1	110.5	73.6	111	0	5798	282	978	116648	3159	459489
18	0.10548	0.00368	0.01579	0.00018	0.33	0.04804	0.00170	101.8	3.4	101.0	1.1	101.0	81.6	81	0	3905	189	459	46953	2097	312493
19	0.10001	0.00375	0.01567	0.00020	0.34	0.04799	0.00183	96.8	3.5	100.2	1.3	97.4	89.1	41	8	4915	237	479	55383	2782	396486
20	0.11211	0.00850	0.01684	0.00043	0.34	0.04811	0.00371	107.9	7.8	107.6	2.7	104.6	172.9	123	12	3241	157	379	40863	1641	243420
Coffee Creek granite (sample YGR-BV-002)																					
1	0.10266	0.00283	0.01560	0.00015	0.35	0.04723	0.00130	99.2	2.6	99.8	1.0	60.6	64.8	13	0	5609	271	1092	100851	2652	401905
2	0.10351	0.00314	0.01555	0.00017	0.36	0.04863	0.00148	100.0	2.9	99.5	1.1	130.1	69.9	7	3	5318	264	763	77001	2568	382295
3	0.10254	0.00365	0.01562	0.00019	0.34	0.04667	0.00167	99.1	3.4	99.9	1.2	32.4	83.5	0	0	3415	162	453	40592	1598	244494
4	0.11053	0.00282	0.01593	0.00015	0.37	0.05002	0.00126	106.4	2.6	101.9	1.0	195.8	57.7	1	6	17773	907	3764	409591	8271	1247606
5	0.10181	0.00388	0.01540	0.00021	0.36	0.04756	0.00182	98.4	3.6	98.5	1.3	76.6	89.4	0	0	5155	250	920	82488	2477	374615
6	0.10176	0.00651	0.01461	0.00034	0.36	0.04990	0.00325	98.4	6.0	93.5	2.1	190.5	144.7	33	19	3938	200	888	68418	1987	301834
7	0.10201	0.00320	0.01519	0.00017	0.36	0.04828	0.00152	98.6	3.0	97.2	1.1	113.0	72.4	0	8	10314	506	1247	163869	5025	759997
8	0.10238	0.00573	0.01540	0.00030	0.35	0.04787	0.00271	99.0	5.3	98.5	1.9	91.6	130.0	0	14	3232	157	468	38180	1556	234992
9	0.10402	0.00369	0.01549	0.00020	0.36	0.04827	0.00172	100.5	3.4	99.1	1.2	112.4	81.8	0	10	5025	246	897	79070	2401	363308
10	0.10591	0.00834	0.01557	0.00044	0.36	0.04749	0.00379	102.2	7.7	99.6	2.8	73.3	180.4	13	14	3131	150	458	41514	1447	225312
11	0.10601	0.00512	0.01550	0.00028	0.37	0.05055	0.00247	102.3	4.7	99.2	1.8	220.2	109.3	0	24	7264	372	1020	110609	3571	525287
12	0.10577	0.00755	0.01605	0.00039	0.34	0.04953	0.00359	102.1	6.9	102.6	2.5	173.0	160.7	0	32	1842	92	252	28766	889	128710

APPENDIX 1 (continued): LA-ICP-MS data for U-Pb analysis of zircons

Fraction	Isotopic Ratios							Isotopic Ages						Background corrected mean counts per second at specified mass							
	$^{207}Pb/^{235}U$	% 1σ	$^{206}Pb/^{238}U$	% 1σ	rho	$^{207}Pb/^{206}Pb$	% 1σ	$^{207}Pb/^{235}U$	± 1σ	$^{206}Pb/^{238}U$	± 1σ	$^{207}Pb/^{206}Pb$	± 1σ	202	204	206	207	208	232	235	238
13	0.10266	0.00535	0.01556	0.00027	0.33	0.04777	0.00251	99.2	4.9	99.5	1.7	86.9	121.1	0	0	1877	90	222	24641	901	135331
14	0.10448	0.00529	0.01566	0.00027	0.34	0.04837	0.00247	100.9	4.9	100.2	1.8	117.5	116.2	0	0	2600	127	437	42164	1242	186288
15	0.10965	0.00332	0.01541	0.00017	0.36	0.05158	0.00155	105.6	3.0	98.6	1.1	266.9	67.5	15	0	8753	456	1268	119562	4250	637230
16	0.10322	0.00458	0.01583	0.00025	0.36	0.04664	0.00208	99.7	4.2	101.2	1.6	30.7	103.6	0	15	7782	366	1603	142208	3631	552001
17	0.10932	0.00805	0.01669	0.00042	0.34	0.04707	0.00350	105.3	7.4	106.7	2.7	52.6	168.7	0	13	2355	111	322	30476	1048	158469
18	0.10110	0.00380	0.01521	0.00020	0.35	0.04749	0.00178	97.8	3.5	97.3	1.3	73.1	87.5	0	5	4880	233	737	60813	2368	360274
19	0.10261	0.00326	0.01576	0.00018	0.36	0.04728	0.00149	99.2	3.0	100.8	1.1	62.9	73.7	30	0	7450	354	1101	99325	3548	530908
20	0.10476	0.00421	0.01544	0.00022	0.35	0.04799	0.00193	101.2	3.9	98.8	1.4	97.5	93.7	0	1	10566	509	3189	295478	5004	769069
Coffee Creek granite (sample 99M-105)																					
1	0.10339	0.00320	0.01534	0.00017	0.36	0.04825	0.00143	99.9	3.0	98.1	1.1	111.5	68.4	0	16	11731	580	1990	189507	6334	877776
2	0.10474	0.00312	0.01561	0.00017	0.37	0.04869	0.00138	101.1	2.9	99.8	1.1	132.9	65.2	0	18	20315	1013	3402	333788	10921	1493286
3	0.10824	0.00361	0.01599	0.00020	0.38	0.04963	0.00160	104.4	3.3	102.3	1.2	177.9	73.3	0	6	9917	504	2341	221170	5256	711046
4	0.24398	0.00746	0.03458	0.00039	0.37	0.05149	0.00148	221.7	6.1	219.2	2.4	263.0	64.5	10	20	29189	1538	3079	150998	7117	967439
5	0.10150	0.00486	0.01481	0.00025	0.35	0.04846	0.00231	98.2	4.5	94.8	1.6	121.7	108.4	0	0	3906	193	564	55271	2151	301957
6	0.10009	0.00494	0.01512	0.00027	0.36	0.04837	0.00238	96.9	4.6	96.8	1.7	117.6	112.0	0	0	3919	193	466	45604	2183	296540
7	0.10281	0.00351	0.01514	0.00019	0.37	0.04824	0.00158	99.4	3.2	96.8	1.2	111.0	75.7	31	0	7273	358	1100	109392	3932	549627
8	0.10453	0.00407	0.01566	0.00022	0.36	0.04954	0.00188	101.0	3.8	100.1	1.4	173.3	86.5	0	0	5663	286	1160	106371	3091	413592
9	0.10374	0.00325	0.01577	0.00018	0.36	0.04777	0.00141	100.2	3.0	100.9	1.1	86.8	69.7	0	13	20375	992	4707	441060	10790	1474918
10	0.10281	0.00406	0.01532	0.00022	0.36	0.04854	0.00187	99.4	3.7	98.0	1.4	125.9	88.1	0	0	8598	425	1609	154907	4667	640612
11	0.10473	0.00366	0.01558	0.00020	0.37	0.04814	0.00161	101.1	3.4	99.6	1.3	106.3	77.4	32	20	9424	462	2090	193303	4977	690328
12	0.10300	0.00375	0.01585	0.00021	0.36	0.04675	0.00164	99.5	3.5	101.4	1.3	36.4	82.0	74	14	6636	315	1111	107044	3459	477455
13	0.10514	0.00529	0.01556	0.00028	0.36	0.04927	0.00246	101.5	4.9	99.6	1.8	160.6	112.7	62	20	3412	170	494	50443	1833	249767
14	0.10278	0.00433	0.01529	0.00023	0.36	0.04895	0.00202	99.3	4.0	97.8	1.5	145.7	93.8	74	0	8571	426	1615	149740	4678	638081
15	0.10584	0.00406	0.01537	0.00021	0.36	0.04909	0.00182	102.1	3.7	98.3	1.4	151.9	84.7	26	16	8694	433	1310	122623	4619	643845
16	0.10492	0.00525	0.01590	0.00028	0.35	0.04809	0.00238	101.3	4.8	101.7	1.8	103.5	113.0	0	0	4775	233	710	74355	2505	341546
17	0.10861	0.00392	0.01521	0.00020	0.36	0.05174	0.00178	104.7	3.6	97.3	1.3	273.9	77.1	6	27	20121	1055	6714	612504	10958	1502498
18	0.10907	0.00461	0.01528	0.00023	0.36	0.05120	0.00211	105.1	4.2	97.8	1.5	249.7	92.1	0	12	4319	224	736	67610	2316	320953
19	0.10310	0.00423	0.01568	0.00023	0.36	0.04662	0.00185	99.6	3.9	100.3	1.5	29.9	92.8	0	27	5749	271	821	76380	2969	416182
20	0.10622	0.00358	0.01585	0.00019	0.36	0.04821	0.00153	102.5	3.3	101.4	1.2	109.4	73.2	89	0	61019	2978	22748	2E+06	31613	4368048
Coffee Creek granite (sample 99M-107)																					
1	0.10349	0.00143	0.01561	0.00009	0.42	0.04802	0.00067	100.0	1.3	99.9	0.6	98.9	34.0	45	13	19926	969	3667	404003	10955	1804307
2	0.11027	0.00158	0.01609	0.00009	0.39	0.04912	0.00072	106.2	1.5	102.9	0.6	153.7	33.8	0	0	17501	871	1841	208355	9242	1537814
3	0.10469	0.00139	0.01552	0.00009	0.44	0.04834	0.00065	101.1	1.3	99.3	0.6	115.9	31.6	10	20	27749	1359	7450	900778	15197	2526153
4	0.10338	0.00288	0.01559	0.00016	0.37	0.04798	0.00137	99.9	2.7	99.7	1.0	97.1	67.3	12	0	9618	467	2576	282684	5296	871889
5	0.10283	0.00146	0.01548	0.00009	0.41	0.04811	0.00069	99.4	1.3	99.1	0.6	104.9	33.7	0	21	25962	1265	4034	451622	14426	2368088
6	0.10297	0.00097	0.01559	0.00007	0.48	0.04778	0.00045	99.5	0.9	99.7	0.4	87.6	23.4	21	1	39500	1911	6471	706364	21778	3577980
7	0.10589	0.00156	0.01541	0.00009	0.40	0.04897	0.00073	102.2	1.4	98.6	0.6	146.3	34.8	0	23	18733	929	2609	312858	10297	1716416
8	0.10197	0.00140	0.01539	0.00009	0.43	0.04788	0.00067	98.6	1.3	98.4	0.6	92.3	33.8	0	12	27552	1335	6336	702124	15385	2527561
9	0.10126	0.00409	0.01529	0.00022	0.36	0.04708	0.00194	97.9	3.8	97.8	1.4	53.1	96.0	108	0	4816	229	834	91738	2665	444486
10	0.10266	0.00167	0.01534	0.00010	0.40	0.04808	0.00080	99.2	1.5	98.1	0.6	103.2	38.8	42	44	20654	1005	3880	471386	11518	1899842
11	0.10328	0.00146	0.01547	0.00009	0.41	0.04807	0.00069	99.8	1.3	98.9	0.6	102.8	33.6	43	0	22228	1081	2748	308437	12325	2026927
12	0.10122	0.00108	0.01547	0.00007	0.42	0.04706	0.00051	97.9	1.0	98.9	0.5	51.9	25.0	0	2	29494	1404	4534	532727	16343	2689094
13	0.10438	0.00210	0.01548	0.00012	0.39	0.04815	0.00099	100.8	1.9	99.0	0.8	106.9	47.8	32	0	9946	484	2369	275786	5474	905511
14	0.11169	0.00206	0.01528	0.00011	0.39	0.05171	0.00098	107.5	1.9	97.8	0.7	272.4	42.7	57	12	24701	1291	3507	402829	13647	2278058
15	0.10378	0.00144	0.01549	0.00009	0.42	0.04793	0.00067	100.3	1.3	99.1	0.6	94.6	34.1	18	10	29880	1448	4300	484201	16476	2717852
16	0.10438	0.00118	0.01533	0.00008	0.46	0.04857	0.00056	100.8	1.1	98.1	0.5	127.1	26.8	0	31	28842	1416	4683	531450	16031	2649627
17	0.10634	0.00789	0.01581	0.00041	0.35	0.04827	0.00366	102.6	7.3	101.1	2.6	112.3	170.0	0	22	2477	120	433	51036	1344	220623
18	0.10302	0.00349	0.01537	0.00019	0.36	0.04778	0.00166	99.6	3.2	98.3	1.2	87.3	81.2	62	8	4966	239	1028	121390	2754	454978
19	0.10650	0.00165	0.01558	0.00010	0.41	0.04796	0.00075	102.8	1.5	99.7	0.6	96.3	38.0	0	0	26515	1285	5199	589256	14289	2394737
20	0.10789	0.00175	0.01591	0.00010	0.39	0.04794	0.00079	104.0	1.6	101.8	0.7	95.0	39.8	71	15	17309	838	1980	206543	9207	1530508
SUBVOLCANIC ROCKS																					
Quartz-feldspar rhyodacite porphyry (sample MA11-001BV)																					
1	0.07309	0.01078	0.00875	0.00038	0.29	0.05832	0.00880	71.6	10.2	56.2	2.4	541.0	300.5	0	0	494	28	106	18700	364	82084
2	0.05686	0.00399	0.00887	0.00022	0.35	0.04567	0.00328	56.2	3.8	56.9	1.4	0.1	145.3	33	0	1799	82	367	81481	1336	295312
3	0.04568	0.01112	0.00885	0.00044	0.20	0.03531	0.00869	45.4	10.8	56.8	2.8	0.1	0.0	0	26	512	18	115	24413	366	84420
4	0.05088	0.00764	0.00925	0.00033	0.24	0.03949	0.00601	50.4	7.4	59.3	2.1	0.1	0.0	0	0	921	36	216	47781	662	145440
5	0.06909	0.01472	0.00869	0.00052	0.28	0.06103	0.01331	67.8	14.0	55.8	3.3	640.3	410.5	11	0	337	20	52	14286	276	56818
6	0.07700	0.02564	0.01119	0.00103	0.28	0.05967	0.02033	75.3	24.2	71.7	6.5	591.7	605.3	0	0	249	14	58	13033	179	32723
7	0.05696	0.01555	0.00940	0.00057	0.22	0.04050	0.01119	56.2	14.9	60.3	3.6	0.1	271.6	0	0	452	18	88	18221	299	70736

APPENDIX 1 (continued): LA-ICP-MS data for U-Pb analysis of zircons

Fraction	Isotopic Ratios							Isotopic Ages						Background corrected mean counts per second at specified mass							
	$^{207}Pb/^{235}U$	% 1σ	$^{206}Pb/^{238}U$	% 1σ	rho	$^{207}Pb/^{206}Pb$	% 1σ	$^{207}Pb/^{235}U$	± 1σ	$^{206}Pb/^{238}U$	± 1σ	$^{207}Pb/^{206}Pb$	± 1σ	202	204	206	207	208	232	235	238
8	0.05539	0.00704	0.00899	0.00030	0.26	0.04413	0.00570	54.7	6.8	57.7	1.9	0.1	187.3	0	0	966	42	191	47019	716	158022
9	0.05015	0.01224	0.00905	0.00040	0.18	0.03881	0.00955	49.7	11.8	58.1	2.6	0.1	117.1	23	0	493	19	101	21635	355	80214
10	0.04233	0.01804	0.00865	0.00051	0.14	0.03604	0.01545	42.1	17.6	55.5	3.3	0.1	263.1	41	41	253	9	51	15566	201	43204
11	0.05107	0.00825	0.00916	0.00032	0.22	0.03957	0.00646	50.6	8.0	58.8	2.0	0.1	0.0	4	0	648	25	120	28156	469	104654
12	0.08295	0.03003	0.00850	0.00072	0.23	0.06746	0.02488	80.9	28.2	54.6	4.6	852.1	622.2	40	8	188	12	54	10182	143	32829
13	0.05907	0.00569	0.00875	0.00027	0.32	0.04902	0.00483	58.3	5.5	56.1	1.7	149.0	216.0	61	3	1224	60	173	36942	950	207605
14	0.06656	0.01159	0.00844	0.00039	0.27	0.05989	0.01064	65.4	11.0	54.2	2.5	599.6	344.2	18	2	399	23	61	17326	336	70346
15	0.06503	0.00747	0.00895	0.00033	0.32	0.05622	0.00663	64.0	7.1	57.4	2.1	460.2	242.9	0	13	763	43	103	21803	618	126965
16	0.05293	0.00944	0.00945	0.00045	0.27	0.04176	0.00758	52.4	9.1	60.6	2.9	0.1	163.7	44	16	1003	42	170	41699	743	158430
17	0.05040	0.00656	0.00856	0.00027	0.24	0.04180	0.00552	49.9	6.4	54.9	1.8	0.1	64.9	0	0	855	35	67	19465	666	149306
18	0.06156	0.00602	0.00910	0.00023	0.26	0.04869	0.00483	60.7	5.8	58.4	1.5	133.0	217.8	0	0	957	46	131	29664	712	157333
19	0.03562	0.01216	0.00817	0.00038	0.14	0.03120	0.01071	35.5	11.9	52.4	2.5	0.1	0.0	0	0	433	13	118	21499	357	79560
20	0.06905	0.00647	0.00908	0.00028	0.33	0.05667	0.00544	67.8	6.2	58.3	1.8	477.9	200.1	4	20	882	50	230	43210	682	145736